Biogeosciences Discussions
Article In Press
Acceptation date : January 2018
http://dx.doi.org/10.5194/bg-2017-559
http://archimer.ifremer.fr/doc/00419/53042/

Modelling the processes driving *Trichodesmium* sp. spatial distribution and biogeochemical impact in the tropical Pacific Ocean

Dutheil Cyril [1, 2, *], Aumont Olivier [2], Gorguès Thomas [3], Lorrain Anne [4], Bonnet Sophie [5], Rodier Martine [6], Dupouy Cécile [5], Shiozaki Takuhe [7], Menkes Christophe [1, 2]

[1] Centre IRD, Nouméa, New Caledonia
[2] LOCEAN Laboratory, IPSL, Sorbonne Universités (UPMC, Univ Paris 06)-CNRS-IRD-MNHN, Paris, France
[3] Laboratoire d'Océanographie Physique et Spatiale (LOPS), Univ. Brest-CNRS-Ifremer-IRD, Plouzané, France
[4] LEMAR, UMR 6539, UBO-CNRS-Ifremer-IRD, IUEM, Plouzané, France
[5] Aix Marseille Université, CNRS/INSU, Université de Toulon, IRD, Mediterranean Institute of Oceanography (MIO) UM 110, 13288, Marseille, France
[6] Environnement Insulaire Océanien (EIO), UMR 241 (Univ. de Polynésie Française, IRD, ILM, IFREMER), Tahiti, French Polynesia
[7] Research and Development Center for Global Change, Japan Agency for Marine-Earth Science and Technology, Yokosuka, Japan

* Corresponding author : Cyril Dutheil, email address : cyril.dutheil@ird.fr

Abstract :

Dinitrogen fixation is now recognized as one of the major sources of bio-available nitrogen in the ocean. Thus, nitrogen fixation sustains a significant part of the global primary production by providing an input of the most common limiting nutrient for phytoplankton growth. Evidences of the Western Tropical South Pacific being a hotspot of nitrogen fixation, and a data coverage complemented by OUTPACE, lead us to develop an explicit nitrogen fixation compartment based on the *Trichodesmium* physiology (the most studied nitrogen fixer) within a 3D coupled dynamical-biogeochemical model (ROMS-PISCES). We performed a first 20-year tropical Pacific simulation that is able to reproduce the main physical (e.g. Sea Surface Temperature) and biogeochemical conditions (nutrients, and chlorophyll concentrations as well as dinitrogen fixation). This simulation showed a possible *Trichodesmium* regional distribution that extends from 150° E to 120° W in the south tropical Pacific, and from 120° E to 140° W in the north tropical Pacific. The local simulated maximums were around islands (Hawaii, Fiji, Samoa, New Caledonia, Vanuatu). We assessed that 15 % of the total primary production may be due to *Trichodesmium* in the Low Nutrient, Low Chlorophyll regions (LNLC). We also argue that implicit parameterization of N_2 fixation (often used in biogeochemical models) leads to underestimate nitrogen fixation rates by about 25% in LNLC regions compared to our explicit formulation. Finally, we showed that iron fluxes from island sediments control the spatial distribution and the abundance of

Trichodesmium in the western tropical south Pacific. Noteworthy, this last result does not take into account the iron supply from rivers and hydrothermal sources, which may well be of importance in a region known for its strong precipitation rates and volcanic activity.

1. Introduction

Nitrogen is known to be the most common limiting nutrient for phytoplankton growth in the modern world ocean (Moore et al., 2013), especially in the Low Nutrient, Low Chlorophyll (LNLC) ecosystems (Arrigo, 2005; Gruber, 2005). Characterizing the processes governing nitrogen sources and sinks to and from the ocean is therefore central to understanding oceanic production, organic matter export and food web structure. Atmospheric dinitrogen (N_2) dissolved in seawater is by far the dominant form of N present in the ocean, i.e. the N_2:NO_3^- ratio typically exceeds 100 in surface waters. However, most phytoplankton species cannot assimilate N_2, and grow using reactive forms of nitrogen such as nitrate, ammonium and dissolved organic compounds. Some planktonic prokaryotic microorganisms, called "diazotrophs" use an enzyme, the nitrogenase, to fix N_2 and convert it into ammonia (NH_3) and ultimately ammonium (NH_4^+). At the global scale, they provide the major external source of reactive nitrogen to the ocean (Gruber, 2008), and support up to 50% of new production in tropical and subtropical (LNLC) regions (Bonnet et al., 2009; Capone, 1997; Deutsch et al., 2007; Karl et al., 1997; Moutin et al., 2008; Raimbault and Garcia, 2008). These organisms are physiologically and taxonomically diverse including cyanobacteria, bacteria, archaea (Zehr and Bombar, 2015; Delmont et al., 2017)(Delmont et al., 2017; Zehr and Bombar, 2015).

Autotrophic diazotrophs have been far more intensively studied than heterotrophic diazotrophs, whose contribution to global N_2 fixation remains unclear (Turk-Kubo et al., 2014; Bombar et al., 2016; Moisander et al., 2017)(Bombar et al., 2016; Moisander et al., 2017; Turk-Kubo et al., 2014). Autotrophic diazotrophs have been characterized both in the field and through laboratory experiments and their physiology is consequently better (Bergman et al., 2013; Küpper et al., 2008; Mulholland et al., 2001; Mulholland and Capone, 2000; Ohki et al., 1992; Ramamurthy and Krishnamurthy, 1967; Rubin et al., 2011). Cyanobacterial (autotrophic) diazotrophs are composed of 3 main groups: 1) the filamentous diazotrophs including the colonial, non-heterocyst-forming *Trichodesmiu*m, 2) the heterocyst-forming symbionts associated with diatoms (DDAs), and 3) the unicellular cyanobacterial diazotrophs (UCYN, phylogeneticaly divided into three groups :, UCYN-A, B, and C). It has been established that autotrophic diazotrophs growth rates are typically one order of magnitude lower than those of non-diazotrophs (Breitbarth et al., 2008; Falcón et al., 2005; Goebel et al., 2008; LaRoche and Breitbarth, 2005). This can be related to the high energetic demand (Postgate, 1982) required to convert N_2 to NH_3 as compared to that necessary to assimilate nitrate or ammonia. This low growth rate (compared to other phytoplankton species) mainly constrains their ecological niches to nitrate-poor regions, where they can be competitive. Moreover, their geographical distribution is constrained by nutrient availability in the photic layer (mainly iron and phosphate) (Berman-Frank, 2001; Bonnet et al., 2009; Mills et al., 2004; Moutin et al., 2005, 2008; Rubin et al., 2011; Rueter, 1988) and temperature (Staal et al., 2003). Trichodesmium sp. are present only in water where temperature is above 20°C (Capone, 1997; LaRoche and Breitbarth, 2005; Montoya et al., 2004), while some UCYN can be found in colder and deeper waters (Bonnet et al., 2015a; Church et al., 2005; Moisander et al., 2010)

The spatial distribution and rates of N_2 fixation have been inferred at the global scale using several tools. (Deutsch et al., 2007) have introduced the tracer P* which represents the excess of P relative to the standard N quota. A decrease in this tracer is then interpreted as N_2 fixation, since N_2 fixation extracts PO_4 alone. More recently, (Luo et al., 2014)

developed a multiple linear regression that relates N_2 fixation from the MAREDAT database (Luo et al., 2012) to environmental conditions (nutrients, SST, irradiance, MLD,...) in order to build a statistical model for global N_2 fixation distribution. Finally, numerical models have also been used and they allow to overcome the scarcity of observations that may limit the two previous approaches. Indeed, models can be used to investigate the spatial and temporal variability of dinitrogen fixation and to study the controlling environmental factors.

Among those studies focusing on the spatial distribution of dinitrogen fixation, (Berthelot et al., 2017; Bonnet et al., 2009, 2015a; Garcia et al., 2007; Shiozaki et al., 2014) based on oceanographic campaigns have reported high N_2 fixation rates in the Western Tropical South Pacific (WTSP), that has been recently identified as a globally important hot spot of N_2 fixation with rates > 600 µmol N $m^{-2}.d^{-1}$ (Bonnet et al., 2017). Very high abundances of Trichodesmium have been historically reported in this region (Dupouy et al., 2000, 2011; Moisander et al., 2008; Neveux et al., 2006; Shiozaki et al., 2014); Stenegren et al., This issue) and have recently been identified as the major contributor to N_2 fixation in this region (Berthelot et al., 2017); Bonnet et al., This issue). However, the reasons for such an ecological success of diazotrophs in this region are still poorly understood.

In this study, we aim at bringing new insights on this known, but poorly understood, "nitrogen fixation hotspot". This study ambitions to understand the spatial and temporal distribution (i.e. seasonal variability) o*f Trichodesmiu*m and to evaluate the potential impact o*f Trichodesmiu*m fixers on the biogeochemical conditions of the WTSP. We will specifically address the following overarching questions: (i) What are the mechanisms that structure the *Trichodesmium* distribution in the WTSP, particularly around the South West Pacific islands, and (ii) what is the biogeochemical impact of N_2 fixation in this region? Noteworthy, this study is also taking advantage of the sampling done during the OUTPACE cruise, which nicely complement the data coverage in the south west Pacific, and allow a better characterization of the processes responsible for the spatial and seasonal variability of the N_2 fixation.

To fulfill our objectives, we have implemented an explicit representation of the nitrogen fixers in a biogeochemical model, based on the *Trichodesmium* physiology. The first section of this study describes the experimental design and the observation used in our study, while the second part of the paper provides a validation of our reference simulation with an analysis of the *Trichodesmium* compartment and its impacts on the biogeochemical conditions of the Tropical Pacific. In the discussion, the impact of iron from islands sediment on dinitrogen fixation is considered as well as the added value of an explicit dinitrogen fixer compartment rather than a simpler implicit representation of dinitrogen fixation. Finally, implications and limits of our modeling exercise are detailed in the conclusion.

2. Methods

2.1 Coupled dynamical (ROMS)-primary production (PISCES) model

In this study, we used a coupled dynamical-biogeochemical framework based on the regional ocean dynamical model ROMS (Regional Oceanic Modeling System, (Shchepetkin and McWilliams, 2005) and the state of the art biogeochemical model PISCES (Pelagic Interactions Scheme for Carbon and Ecosystem Studies). The ocean model configuration is based on the nested version of ROMS (Penven et al., 2006) and covers the tropical Pacific region [33°S-33°N;110°E-90°W]. It has 41 terrain-following vertical levels with 2-5 m vertical resolution in the top 50 meters of the water column, then 10-20 m resolution in the thermocline and 200-1000 m resolution in the deep ocean. The

horizontal resolution is 1°. The turbulent vertical mixing parameterization is based on the non-local K profile parameterization (KPP) of (Large et al., 1994). Open boundary conditions are treated using a mixed active/passive scheme (Marchesiello et al., 2001). This scheme allows to force our regional configuration with large-scale boundary conditions from a ½° global model simulation (details available in (Couvelard et al., 2008), while allowing anomalies to radiate out of the domain. The use of similar ROMS configurations in the WTSP is largely validated through studies demonstrating skills in simulating both the surface (Jullien et al., 2012, 2014; Marchesiello et al., 2010) and subsurface ocean circulation (Couvelard et al., 2008). To compute the momentum and fresh water/heat fluxes, we use a climatological forcing strategy. The momentum forcing is computed from a 1993-1996 7-day climatology of the ERS1-2 scatterometer stress (http://cersat.ifremer.fr/oceanography-from-space/our-domains-of-research/air-sea-interaction/ers-ami-wind). Indeed, ERS derived forcing has been shown to produce adequate simulations of the Pacific Ocean dynamics (e.g, (Cravatte et al., 2007). Heat and fresh water forcing is computed from the COADS climatology 1-day averaged outputs are stored for analysis. ROMS forces on line a biogeochemical model with the noticeable use of a WENO5 advection scheme (i.e. five order weighted essentially non-oscillatory scheme; Shchepetkin and McWilliams, 1998).

The biogeochemical model PISCES simulates the marine biological productivity and the biogeochemical cycles of carbon and the main nutrients (P, N, Si, Fe) (Aumont and Bopp, 2006a). In PISCES, there are five modeled limiting nutrients for phytoplankton growth: nitrate, ammonium, phosphate, silicate and iron. Those nutrients are delivered to the ocean through dust deposition, river runoff and mobilization from the sediment. In addition to the nutrients, Dissolved Inorganic Carbon (DIC), total alkalinity and dissolved oxygen are also simulated. Three non-living organic compartments are represented: semi-labile dissolved organic matter, small sinking particles, and large sinking particles. In this study, we used a modified version of PISCES which differs in the use of a full quota formulation (with only variable Redfield ratios; (Droop, 1983) rather than the mixed Monod-quota approach (with fixed ratios for nitrogen, phosphorus and silica; Monod, 1942) used in the standard PISCES version (Aumont and Bopp, 2006). In this "quota" version of PISCES (Kwiatkowski et al, 2017, submitted), the phytoplankton growth is limited by the internal availability in nutrients. For the purpose of this study, we also implemented in this quota version an explicit representation of Trichodesmium. Therefore, five living compartments are modeled with three phytoplankton groups (nanophytoplankton, diatoms, and *Trichodesmium*) and two zooplankton groups (microzooplankton, and mesozooplankton).

In our configuration, the growth rate of *Trichodesmium* is limited by light, temperature, phosphorus and iron availability. *Trichodesmium* growth rate is computed as follows:

Growth rate = ($\mu FixN_2 + \mu TriNO_3 + \mu TriNH_4$),

where $\mu FixN_2$ denotes growth due to dinitrogen fixation, $\mu TriNO_3$ and $\mu TriNH_4$ represent growth sustained by NO_3^- and NH_4^+ uptake, respectively. Dinitrogen fixation is activated when reactive nitrogen species are limiting. Otherwise, *Trichodesmium* grows on NO_3^- and NH_4^+ just like standard nanophytoplankton do. Moreover, a fraction of fixed nitrogen is released by the simulated Trichodesmium. (Berthelot et al., 2015) estimated this fraction at less than 10% while considering all diazotrophs. Because we are only representing Trichodesmium, we set up this fraction at 5% of total amount of fixed nitrogen.

Dinitrogen fixation is controlled by the availability of phosphate, iron and light and is modulated by temperature. The complete set of equations of *Trichodesmium* is detailed in Appendix 1. This setup reproduces the dinitrogen fixation through an explicit representation of the Trichodesmium biomass (to be compared with often used implicit parameterization that links directly environmental parameters to nitrogen fixation without requiring the Trichodesmium

biomass to be simulated).

2.2 Setup of experiments

Below are summarized the set of experiments that have been performed in this study (Table 1). A first simulation over 20-years (1993-2013) has been performed as a reference experiment, hereafter referred to as "TRI". This reference simulation uses the explicit dinitrogen fixation module described above. In a second experiment called "TRI_NoFeSed", the model setup is identical to the reference experiment, except that iron input from the sediments is turned off between 156°E and 240°E. In a third experiment "N2_imp", the explicit dinitrogen fixation module is replaced by the implicit parameterization described in (Aumont et al., 2015). Finally, a fourth experiment "N2_Wo" corresponds to a model setup in which no explicit nor implicit description of dinitrogen fixation is activated. Comparison between TRI and TRI_NoFeSed experiments allow to estimate the impact of iron input from island sediments on the dinitrogen fixation, while the impact of dinitrogen fixation on the biogeochemical conditions in the Pacific Ocean can be investigated by comparing TRI and N2_Wo. Finally, the TRI and N2_imp experiments are used to evaluate the added value of an explicit description of dinitrogen fixation relative to an implicit inexpensive parameterization.

2.3 Observational datasets.

Several different databases have been used to evaluate the model skills. For nitrate and phosphate, the CSIRO ½° global Atlas of Regional Seas (CARS, http://www.marine.csiro.au/~dunn/cars2009/) has been used. Iron has been evaluated with the global database from (Tagliabue et al., 2012), to which the dissolved iron data from the OUTPACE cruise (Guieu et al., under review) have been added. This database is a compilation of 13125 dissolved iron observations covering the global ocean and encompassing the period 1978–2008. The global MARine Ecosytem DATa (MAREDAT, https://doi.pangaea.de/10.1594/PANGAEA.793246) database of N_2 fixation has been expanded with data from recent cruises performed in the WTSP (MOORSPICE, (Berthelot et al., 2017), DIAPALIS ((Garcia et al., 2007), NECTALIS (http://www.spc.int/oceanfish/en/ofpsection/ema/biological-research/nectalis), PANDORA (Bonnet et al., 2015a), OUTPACE (Bonnet et al., This issue), Mirai (Shiozaki et al., 2014) has been used for dinitrogen fixation rates. This database contains 3079 data points at the global ocean scale, of which ~1300 are located in our simulation region (Luo et al., 2012). Finally, we have used surface chlorophyll concentrations from the GLOBCOLOUR project (http://ftp.acri.fr) which spans the 1998-2013 time period.

3.Results

3.1 Model Validation

In this subsection, we aim at validating our reference simulation "TRI" with the data previously mentioned. In the Pacific, phosphate and nitrate concentrations show maxima in the upwelling regions, i.e. along the western American coast, and in the equatorial upwelling (Fig. 1a,c), and mimima in the subtropical gyres. First, phosphate patterns show

193 modeled values and structures in qualitatively good agreement with observations. In contrast, the nitrate structure shows
194 some biases. We observe concentrations higher than 1 µmol.L^{-1} all along the equator in CARS, while in the model
195 nitrate concentrations are lower than this value west of 170W°. More generally the model tends to underestimate nitrate
196 concentrations.
197 The regions most favorable for *Trichodesmium* can be defined by temperature within 26-29°C. The model reproduces
198 relatively well the spatial distribution of this temperature preferendum. This distribution exhibits a significant seasonal
199 variability, mainly as a result of the variability of the 26°C isotherm. The latter moves by ~5° latitudinally between
200 summer and winter in the WTSP, and by ~15° in the Western Tropical North Pacific (WTNP) (Fig. 1a). Along the
201 equator, this isotherm migrates by 15° eastward during summer (Fig. 1a). This temporal variability is well reproduced
202 by the model (Fig. 1b). In contrast, nitrate and phosphate seasonal variability remains low (not shown).
203 Another important feature that needs to be properly reproduced by the model is the iron distribution in the upper ocean.
204 The median value as well as the dispersion of the iron surface concentrations over the tropical Pacific, are displayed for
205 both the data and the model in Figure 2a. No statistical differences can be distinguished, the model being sampled at the
206 same time and same location as the data. This latter result shows a good agreement between the data and the model at
207 the tropical Pacific scale (Fig 2b compared to Fig. 2c). The best sampled area is the central Pacific ocean where
208 simulated iron concentrations are low (0.1 to 0.3 nmol $Fe.L^{-1}$), which is consistent with the observations. The southwest
209 Pacific is characterized by relatively high surface iron concentrations, between 0.4 and 0.8 nmol $Fe.L^{-1}$, both in the data
210 and in the model. Large scale patterns are thus well represented by the model. Nevertheless, the model tends to
211 overestimate iron levels in the south Pacific gyre, between 180° and 140°W at about 20°S.
212 Figure 3 displays a comparison between surface Chlorophyll concentrations from GLOBCOLOUR data (a), and from
213 TRI (b) and TRI_imp (c) simulations. Strong chlorophyll concentrations are found in the eastern equatorial Pacific
214 upwelling and along Peru in both the observations and our 2 simulations, with mean values of 0.3 mg $Chl.m^{-3}$. The
215 equatorial rich tongue simulated by the model (Fig. 3b,c) is however too narrow compared to the observations,
216 especially in the northern hemisphere. Similarly, the model is unable to simulate the elevated chlorophyll levels around
217 the Costa Rica dome and the localized enhanced chlorophyll off Papua New Guinea. In TRI (Fig. 3b), chlorophyll
218 values in the South West Pacific region vary between 0.1 and 0.2 mg $Chl.m^{-3}$, with maxima located in the vicinity of the
219 Fiji and Vanuatu islands. These values are within the range of the data, even if the data tend to be slightly higher (up to
220 0.3 mg $Chl.m^{-3}$ near the coasts). The spatial structure is well represented, with maxima simulated around the islands.
221 Those localized chlorophyll enhancement suggest a specific island effect. In the subtropical gyres, the simulation
222 predicts chlorophyll concentrations of ~0.05 mg $Chl.m^{-3}$ which are higher than the observations (< 0.025 mg $Chl.m^{-3}$).
223 In contrast in TRI_imp (Fig. 3c), chlorophyll values in the South West Pacific and in the North hemisphere are too low
224 in comparison with the ocean colour data (Fig. 3a). TRI simulation thus appears in better agreement with the
225 observations than TRI_imp.
226 Part of the surface chlorophyll in Figure 3b is associated to *Trichodesmium*. The Figure 3d shows the annual mean
227 spatial distribution of surface Trichodesmium chlorophyll in the "TRI" simulation. This distribution displays two zonal
228 tongues in the tropics, one in each hemisphere. Maximum values are located in the South West Pacific (around Vanuatu
229 archipelago, New Caledonia, Fiji, and Papua New Guinea) and around Hawaii, where they reach 0.06 mg $Chl.m^{-3}$. In
230 the south Pacific, high chlorophyll biomass extends eastward until 130°W. Further east, concentrations drop to below
231 0.02 mg $Chl.m^{-3}$. It's important to note that in the observations *Trichodesmium* has never observed beyond 170°W. This
232 bias in the model could be explain by the overestimation of iron concentrations in SPG. In the Northern Hemisphere,
233 between the coast of Philippines (120°E) and Hawaii (140°W), *Trichodesmium* chlorophyll concentrations are greater

than 0.03 mg Chl.m^{-3}. In the North East Pacific, *Trichodesmium* chlorophyll is lower, yet significant (<0.03 mg Chl.m^{-3}). Otherwise the equatorial Pacific and South-east Pacific oceans are overall poor in *Trichodesmium*.

In Figure 4, the dinitrogen fixation rates predicted by the model in "TRI" are compared to the observations from the MAREDAT expanded database. Evaluation of the model behavior remains quite challenging because of the scarcity of the observations. Some large areas are not properly sampled such as the north west tropical Pacific and the eastern Pacific. Nevertheless, some regional patterns emerge from the observations. Maximum fixation rates (~600 to 1600 µmol N.m^{-2}.d^{-1}; Fig. 4a) are observed around the south west Pacific islands, in the Solomon Sea, around the Melanesian archipelagoes and around Hawaii, four well known « hotspots » of N_2 fixation (Berthelot et al., 2015, 2017, Bonnet et al., 2009, 2017; Böttjer et al., 2017). The modeled regional patterns of strong fixation are coherent with the observations (Fig. 4b), showing values in the same range. In the south Pacific, the TRI simulation is able to reproduce the strong east-west increasing gradient of N_2 fixation as reported by dinitrogen fixation (Shiozaki et al., 2014; Bonnet et al., This issue; Fig 4c,d). In the equatorial Central Pacific, modeled values of mean fixation are negligible (< 0.5 µmol N.m^{-2}.d^{-1}) in contrast to the observations which suggest low but non-negligible fixation rates (between 1 to 2 µmol N.m^{-2}.d^{-1}; (Bonnet et al., 2009; Halm et al., 2012). In general, dinitrogen fixation rates are overestimated by ~70% in TRI compared to the data. Some recent studies have shown that the $^{15}N_2$-tracer addition method (Montoya et al., 2004) used in most studies reported in the MAREDAT database may underestimate N_2 fixation rates due to an incomplete equilibration of the $^{15}N_2$ tracer in the incubation bottles, which may explain the differences observed between the modeled and measured rates (Großkopf et al., 2012; Mohr et al., 2010). However, some other studies performed in the South Pacific (Bonnet et al., 2016b; Shiozaki et al., 2015) compared the two methods, and did not found any significant differences.

3.2 Trichodesmium Primary Production

We evaluated the direct relative contribution of *Trichodesmium* to PP (Fig. 6). The spatial distribution of this contribution is very similar to the spatial distribution of *Trichodesmium* chlorophyll, with 2 distinct tongues located on each side of the Equator in the tropical domain. In the Northern hemisphere, the tongue extends from the coast of Philippines (120°E) to Hawaii (140°W) longitudinally and between 10°N and 25°N latitudinally. The maximum contribution (~35%) is reached near Hawaii while in the rest of the tongue, values are close to 20%. In the Southern Hemisphere, the region of elevated contribution extends from PNG (140°E) to about the center of the South Pacific subtropical gyre at 130°W, and between 5°S and 25°S latitudinally. Maximum values are predicted in the vicinity of Vanuatu and Fiji Islands, where they can reach 35%. Part of this elevated contribution is explained by the very low PP rates simulated in this region for both nanophytoplankton and diatoms (less than 0.03 mol C.m^{-3}.yr^{-1}). Furthermore, the island effect seems to represent an important factor for explaining the spatial distribution of *Trichodesmium* growth rates. Indeed, maximum *Trichodesmium* chlorophyll concentrations and the largest contribution of *Trichodesmium* to PP are achieved near the islands. Finally, in LNLC regions (red boxes; fig. 1c,d), we assess that *Trichodesmium* contribute to 15% of total PP, which is in accordance with biogeochemical studies performed in these areas (Bonnet et al., 2015; Berthelot et al., 2017; Caffin et al., This issue)

3.3 Seasonal variability of Trichodesmium biomass

Simulated dinitrogen fixation rates and *Trichodesmium* biomass (not shown) display a seasonal variability that is driven

by the seasonal variability of the environmental conditions (light, temperature, currents, nutrients). The regional maxima of *Trichodesmium* biomass (exceeding 3 mmol $C.m^{-2}$; integrated over the top 100m of the ocean) are found in both hemispheres during the summer season (Fig. 7a,e) even if locally, maxima can be attained during other periods of the year than summer. In the south Pacific, the area of elevated *Trichodesmium* biomass moves by 3° southward from austral winter to austral summer. Along Australia and in the Coral Sea, *Trichodesmium* biomass exhibits a large seasonal variability with very low winter biomass that contrast with elevated values in summer. A similar important variability, which is shifted by six months, is simulated in the Northern hemisphere in the Micronesia region and in the Philippine Sea.

Unfortunately, due to the scarcity of N_2 fixation data over the annual cycle, this seasonal cycle cannot be properly assessed at the scale of the tropical Pacific Ocean. This is only feasible at the time series station ALOHA located in the North Pacific gyre at 22°45',158°W, where seasonal data of dinitrogen fixation are available from 2005 to 2012 (Böttjer et al., 2017). They proved that vertically integrated dinitrogen fixation rates are statistically significantly lower from November to March (less than 200 µmol N $m^{-2}.d^{-1}$) than from April to October (about 263 ± 147 µmol $N.m^{-2}.d^{-1}$) as highlighted in Figure 5a (blue dots). In the model (red dots; Fig. 5a), the maximum amplitude of the seasonal cycle appears to be underestimated relative to the observations (i.e. respectively ~170 µmol $N.m^{-2}.d^{-1}$ and ~250 µmol $N.m^{-2}.d^{-1}$). Dinitrogen fixation peaks one month earlier in the model than in the data (August for the model and September for the data). The simulated dinitrogen fixation rates are minimum between December and May (averaging ~241 ± 27 µmol $N.m^{-2}.d^{-1}$) and maximum the rest of the year (averaging ~ 347 ± 52 µmol $N.m^{-2}.d^{-1}$). These values are comparable to the data even if they are slightly higher.

In order to assess the seasonal cycle of N_2 fixation rates in the south Pacific (red box Fig 1c; 160°E-230°E; 25°S-14°S), we have extracted the available data for each month from our database (blue dots; Fig. 5b), and the corresponding model values in TRI (red dots; Fig 5b). In July no observations are available and in January, April and August, only one data point is available for the entire region. The predicted seasonal cycle is broadly consistent with observations. Minimum dinitrogen fixation rates (239 ± 205 µmol $N.m^{-2}.d^{-1}$) occur during austral winter and autumn. Maximum rates are reached in February and March, where they exceed 600 µmol $N.m^{-2}.d^{-1}$ in the observations. The increase in dinitrogen fixations rates occurs one month earlier than in the observations, in December instead of January, and remains two to three fold higher from April to June. It is important to note here that the sampling spatial and temporal distribution may distort the seasonal cycle. Using the model, it is possible to evaluate how well the seasonal cycle is captured by the sampling (red dots compared to green dots; Figure 5b). The general structure of the seasonal cycle remains relatively unaltered. However, the amplitude is significantly impacted since it reaches 1100 µmol $N.m^{-2}.d^{-1}$ in the sampling whereas it is about twice as low at 600 µmol $N.m^{-2}.d^{-1}$ when all the model data points are considered. We can conclude that the TRI simulation reproduces well the seasonal cycle of N_2 fixation rates at the Pacific scale, even though more data are needed to improve the evaluation of the model skills.

To further investigate the mechanisms that drive the seasonal variability of *Trichodesmium* in the Pacific, we examined the factors that control Trichodesmium abundance in the TRI simulation (not shown). This analysis indicates that this seasonal variability is mainly controlled by primary production. Hence we further examine the limitation terms of primary production (Fig. 8) in two representative regions characterized by elevated levels of N_2 fixation rates (red boxes; Fig 1c). A detailed description of these limitation terms is given in Appendix 1. A limitation term reaching 1 means that growth is not limited whereas a limitation term equal to zero means that growth ceases.

Trichodesmium growth sustained by nitrate and ammonia is very small in LNLC regions due to their very low availability and is therefore not considered further. Thus, our analysis is restricted to dinitrogen fixation. *Trichodesmium*

growth can be limited by iron and phosphate and is inhibited when reactive nitrogen (nitrate and ammonia) is available. In the WTSP, the model suggests that iron is the sole nutrient that modulat*es Trichodesmi*um growth (red curve; Fig. 8a,b). The others limiting factors *of Trichodesmi*um growth are light (green curve; Fig 8a,b) and temperature (purple curve; Fig. 8a,b). The product of these 3 limiting factors gives the limiting coefficient of dinitrogen fixation (brown curve; Fig 8a,b). The limiting factors vary according to the season and the hemisphere. In the south (north) Pacific, temperature and light are less limiting during the austral summer (winter) than during the austral winter (summer). The limiting factor associated to temperature varies from 0.8 to 1, and the light limiting factor varies from 0.15 to 0.3. Unlike light and temperature, iron is less (more) limiting in the south (north) pacific during winter (summer) than during the austral summer (winter) with values varying between 0.4 and 0.7. Finally, *Trichodesmium* growth is more limited during the austral winter (summer) in the south (north) Pacific. The seasonal variability is forced by light and temperature, and iron mitigates its amplitude. Indeed, temperature and iron are anti-correlated because, in the boxes over which this analysis is performed, the ocean dynamic is mainly 1D. Nutrients are thus brought by enhanced vertical mixing which also cools temperature.

4. Discussion

The implementation of dinitrogen fixation in ocean models has become more and more complex over the past twenty years. At first, the supply of new nitrogen by dinitrogen fixation has been embedded into models by developing implicit parameterizations (Bissett et al., 1999). Subsequently explicit descriptions of diazotrophs have been developed, mainly based on the knowledge derived from laboratory experiments focused on Trichodesmium sp. (Fennel et al., 2001; Hood et al., 2001; Moore et al., 2001). Since the mid-2000s, studies focused on the role of iron in controlling the distribution of diazotrophs and dinitrogen fixation (Keith Moore et al., 2006; Krishnamurthy et al., 2009; Moore et al., 2004; Tagliabue et al., 2008).

4.1 Impact of iron from island sediments

Monteiro et al. (2011) and Dutkiewicz et al. (2012) have suggested that a realistic representation of marine iron concentration is key to simulate the diazotrophs habitat. Monteiro et al. (2011) performed a sensitivity study and found that a fivefold increase in the solubility of aeolian iron improves the biogeographical distribution of N_2 fixation in the southwest Pacific. In the meantime, a recent study has challenged this view by showing no increase in dinitrogen fixation in response to increased dust deposition (Luo et al., 2014). In any cases, the sedimentary and hydrothermal sources were not taken into account in those studies, although they are likely significant sources (Bennett et al., 2008; Johnson et al., 1999; Moore et al., 2004; Tagliabue et al., 2010; Toner et al., 2009). In parallel, Dutkiewicz et al. (2012) evaluated the sensitivity of the biogeographical distribution of N_2 fixation to the aeolian source of iron in a model which takes into account the iron sediment supplies, and conclude for minor changes in south west Pacific, while in the north Pacific the change was larger. Indeed, there are many high islands that could deliver significant amounts of iron to the ocean (Radic et al., 2011) in the southwest Pacific.

To assess the impact of the sediment source of iron on the *Trichodesmium* production, we used the "TRI_NoFeSed" experiment in which this specific source of iron has been turned off for the islands between 160°E and 120°W (Table 1).

In this simulation, the iron and the *Trichodesmium* chlorophyll concentrations decrease by 58% and 51% respectively (Fig. 9a,b), in the WTSP (red box Fig 1c). Figure 9c displays the iron distribution simulated in TRI_NoFeSed, and shows that the maximums around the islands disappear. Furthermore, in the south Pacific, iron decreases due to the reduction of the zonal advection of iron downstream of the islands. The iron flux from the sediments around the islands also affects the spatial structure of *Trichodesmium* chlorophyll (Fig. 9d,e), most noticeably in the south Pacific, with maxima shifted from the south Pacific islands region (e.g. Fiji, New Caledonia, Vanuatu) in the TRI simulation to the coastal regions near Australia and Papua New Guinea in the TRI_NoFeSed simulation. In the northern hemisphere, the effects of the sediment flux of iron are less important with a shift of the *Trichodesmium* chlorophyll maxima towards the Philippine Sea and a localized effect near Hawaii. This sensitivity test demonstrates that *Trichodesmium* are highly sensitive to the iron distribution in our model and hence that the spatial patterns of *Trichodesmium* chlorophyll in the south west Pacific are tightly controlled by the release of iron from the coastal sediments of the Pacific islands.

4.2 *Trichodesmium* impacts on biogeochemistry

One of the questions we want to address is the quantification of the *Trichodesmium* impact on primary production (PP), at the Pacific scale with a focus on the WTSP region. In the oligotrophic waters of the south pacific, dinitrogen fixation can be an important source of bio-available nitrogen in the water column through *Trichodesmium* recycling which can feed other phytoplankton. To evaluate that impact, we calculated the relative increase of PP between the TRI simulation and the N2_Wo simulation in which no dinitrogen fixation is considered (Fig 10a). As expected, the spatial structure of the primary production differences between both simulations matches the dinitrogen fixation spatial distribution in the TRI simulation (two tongues, one in each hemisphere). In the north Pacific the maximum increase of the primary production due to the dinitrogen fixation is located around Hawaii, where it exceeds 120%. In the remaining part of the northern hemisphere tongue, primary production increases by 50% to 100%. In the southern hemisphere, values are more homogeneous in the tongue (from 80 to 100%), even though there is a local maximum around Fiji and Vanuatu (up to 120%). Out of these northern and southern tongues, the increase of PP is less than 20%. In average on our domain, the increase of PP is 19% and in LNLC regions, it reaches approximately 50%.

From total primary production only, it is not possible to disentangle the increase of primary production directly due to *Trichodesmium* themselves and the indirect increase due to the impact of dinitrogen fixation on the other phytoplankton groups (nanophytoplankton and diatoms). Indeed, as mentioned in the method section, *Trichodesmium* also releases a fraction of the recently fixed N_2 as bio-available nitrogen (mostly ammonia and dissolved organic nitrogen). Figure 10b displays the difference of PP due to diatoms and nanophytoplankton only. The main large scale patterns constituted of the northern and southern tongues persist, but the intensity of the differences contrasts with those found when considering total primary production (Fig. 10a). Indeed, the increase of total primary production (Fig 10a) in those two tongues is twice as high as when the direct effect *of Trichodesm*ium is excluded. This analysis stresses the importance of the bio-available nitrogen released by diazotrophs as we attribute about half of the total production increase to this release. Indeed, recent isotopic studies tracing the passage of diazotroph-derived nitrogen into the planktonic food web reveal that part of the recently fixed nitrogen is released to the dissolved pool and quickly taken up (24-48%) by surrounding planktonic communities (Berthelot et al., 2016; Bonnet et al., 2016a, 2016b)).

With the simulation N2_imp, we aim at comparing an implicit dinitrogen fixation formulation to the explicit formulation used in TRI. Figure 10c displays the relative change of total PP between the TRI and the N2_imp

simulations (see Table 2). The implicit formulation displays a similar spatial distribution than the explicit distribution but is predicting a lower total primary production, especially in the the southern Pacific where explicit formulation leads to an increase of about 45% in total PP compared to the one related to the implicit formulation. On average across our domain, total primary production is about ~ 9% higher when nitrogen fixation is explicitly modeled relative to an implicit formulation.

This difference becomes even weaker (2%) if only primary production by nanophytoplankton and diatoms is considered, with noticeable differences restricted to the areas of maximum dinitrogen fixation in the southern hemisphere (around the islands). PP sustained by the release of bio-available nitrogen is thus similar in the TRI and N2_imp simulations, but an explicit representation of dinitrogen fixation allows a better description of dinitrogen fixation patterns. Indeed, the areas of intense dinitrogen fixation rates cannot be properly simulated in the vicinity of the islands, especially in the southern hemisphere, by the tested implicit parameterization.

4.3 Limitations

In this study, we simulate dinitrogen fixation through the explicit representation of only one type of diazotrophs, the *Trichodesmium* sp. This choice has been motivated by evidences that it represents one of the main nitrogen fixers in the western tropical Pacific (Bonnet et al., 2015a; Dupouy et al., 2011; Shiozaki et al., 2014) and by the relatively good knowledge (compared to other dinitrogen fixers) we have about its physiology (Ramamurthy and Krishnamurthy, 1967; Ohki et al., 1992; Mulholland and Capone, 2000; Mulholland et al., 2001; Küpper et al., 2008; Rubin et al., 2011; Bergman et al., 2013). However, our model remains simple and some of the mechanisms that drive the behavior of *Trichodesmium* have not been implemented in our model. As an example, the ability of *Trichodesmium* to group in colonies and to vertically migrate (Kromkamp and Walsby, 1992; Villareal and Carpenter, 2003; Bergman et al., 2013) (Bergman et al., 2013; Kromkamp and Walsby, 1992; Villareal and Carpenter, 2003) is well documented. The reason of these mechanisms remains unclear, but several hypotheses have been put forward such as avoiding nitrogenase exposition to di-oxygen (Carpenter, 1972; Gallon, 1992; Paerl et al., 1989), or maximizing light (on the surface) and nutrients (at depth) acquisition (Letelier and Karl, 1998; Villareal and Carpenter, 1990; White et al., 2006), or even increasing the efficiency of the uptake of atmospheric iron (Rubin et al., 2011). Our model does not represent those processes, nor does it model the resulting vertical migration of *Trichodesmium*. Moreover, the release of fixed dinitrogen as reactive nitrogen bioavailable to other phytoplanktonic organisms has been set to a constant value of 5%. This percentage is known to be highly variable and therefore this value is in the lowest range of the observations. An increase in this value would increase the PP due to nanophytoplankton and diatoms in the TRI simulation, and thus decrease the relative contribution of Trichodesmium to total PP, which would be closer to the last observations (Berthelot et al. 2017; Bonnet et al. 2017).

Some studies, mostly based on extrapolated in-situ data, aimed at assessing the potential of dinitrogen fixation at global or regional scale (Codispoti et al., 2001; Deutsch et al., 2001; Galloway et al., 2004). In the western south tropical Pacific, Bonnet et al (2017) have estimated total nitrogen fixation at 15 to 19 Tg $N.yr^{-1}$. For the same region, nitrogen fixation is predicted to amount to ~7 Tg $N.yr^{-1}$ in the TRI simulation. As already mentioned, this rather low predicted estimates might be explained by the sole representation of Trichodesmium as nitrogen fixing organisms, which dominate in the western tropical south Pacific (Dupouy et al., 2011, Stenegren et al., This issue). It has to be noted that other diazotroph groups such UCYN-B and DDAs are abundant in the WTSP, representing 10-20% of the overall

diazotroph community (Stenegren et al., This issue). Moreover, the contribution of heterotrophic diazotrophic organism is poorly studied and may account for a significant fraction of N_2 fixation (Moisander et al., 2017). Our model estimation has also been computed from monthly averages and is thus not taking into account the high-frequency variability that may explain at least some of the very high rates of dinitrogen fixation used in the study by Bonnet et al. (2017). Our assessment based on a model could thus be seen as a lower limit for dinitrogen fixation in the western tropical Pacific. Moreover, our model shows also a good qualitative agreement with the studies based on observations that focus on the impact of dinitrogen fixation in tropical oligotrophic waters (Raimbault and Garcia, 2008; Shiozaki et al., 2013). Indeed, in agreement with those studies, our reference simulation predicts that diazotrophs support a large part of PP (~ 15%) in LNLC regions.

5. Conclusion

This study describes the spatial and temporal distribution of *Trichodesmium* at the scale of the tropical Pacific ocean, and investigates the impact of a major diazotroph species (e.g *Trichodesmium* sp.) on the biogeochemistry of this region. Toward this end, we performed a first 20-year simulation with the coupled 3D dynamical biogeochemical model ROMS-PISCES in which we embedded an explicit representation of dinitrogen fixation based on *Trichodesmium* physiology. This simulation was shown to be able to reproduce the main physical (SST) and biogeochemical (nutrients) conditions of the tropical Pacific ocean. This includes the spatial distribution of surface chlorophyll and dinitrogen fixation.

The validation of this simulation allows us to confidently assess the *Trichodesmium* distribution. The model predicts that areas favorable to *Trichodesmium* growth extend from 150°E to 120°W in the south Pacific, and from 120°E to 140°W in the north Pacific, with local optimal conditions around the islands (i.e., Hawaii, Fiji, Samoa, New Caledonia, Vanuatu). This broadly corresponds to the LNLC regions where Trichodesmium are predicted to be responsible for 15% of total primary production. The seasonal variability of the Trichodesmium habitat is dominantly controlled by SST and light, while iron availability modulates the amplitude of the seasonal cycle.

In our study we also assess the role played by iron released from the island sediments, and show that this iron source partly controls the spatial structure and the abundance of *Trichodesmium* in the western tropical south Pacific. However, this region is in the center of the south Pacific convergence zone which is the largest convective area of the Southern Hemisphere, with rainfall exceeding 6mm.day^{-1}, hence it would be interesting to assess the impact of river iron supply on the diazotrophs activity. In addition, the Vanuatu archipelago and Tonga are located on the ring fire, hence hydrothermal sources could have a strong impact on dinitrogen fixation. These two iron sources are not yet implemented in our configuration but may improve simulations of dinitrogen fixation in the south western tropical Pacific region.Finally, our explicit simulation of dinitrogen fixation has proven to be higher by 25% (while still in the lower end of estimations from observations) than the more commonly used implicit parameterization.

6. Appendix

Trichodesmium preferentially fixes di-nitrogen at temperature between 20-34°C (Breitbarth et al., 2008). The temperature effect on the growth rate is modeled using a 4th order polynomial function (Ye et al., 2012):

$$L_T^{\mathrm{Tri}} = \frac{2{,}32.10^{-5} \times T^4 - 2{,}52.10^{-3} \times T^3 + 9{,}75.10^{-2} \times T^2 - 1{,}58 \times T + 9.12}{0.25}$$

where $0.25 d^{-1}$ is the maximum observed growth rate (Breitbarth et al., 2008). Hence, at 17°C the growth rate is zero and maximum growth rate is reached at 27.5°C.

We first evaluate if nitrate+ammonium limitation occurs. In that case, dinitrogen fixation can occur and it is limited by phosphorus and iron. Phosphorus and iron limitations (L^P, L^{Fe}) are calculated in a 2-step process as follows:

First, we determine the most limiting nutrient:

$$L_{\mathrm{Tri}}^{Fe} = \frac{\left(\theta^{Fe} - \theta_0^{Fe}\right)\theta_{\mathrm{opt}}^{Fe}}{\left(\theta_{\mathrm{opt}}^{Fe} - \theta_0^{Fe}\right)\theta^{Fe}} \quad \text{and} \quad L_{\mathrm{Tri}}^{P} = \frac{\left(\theta^{P} - \theta_{\mathrm{min}}^{P}\right)\theta_{\mathrm{opt}}^{P}}{\left(\theta_{\mathrm{opt}}^{P} - \theta_{\mathrm{min}}^{P}\right)\theta^{P}},$$

where $\theta^{\mathrm{Nutrients}}$ represents the nutrient quota for Fe and PO_4 (i.e, the ratio between iron and carbon concentrations in *Trichodesmium*, for instance).

$$\theta_0^{\mathrm{Fe}} = \theta_{\mathrm{min}}^{\mathrm{Fe}} - m \quad ,$$

where m represents the maintenance iron, the intracellular Fe : C present in the cell at zero net growth rate (Kustka et al., 2003).

$\theta_{\mathrm{min}}^{\mathrm{Nut}}$ and $\theta_{\mathrm{opt}}^{\mathrm{Nut}}$ are constant, whereas θ varies with time. The mimimum of $L^{\mathrm{Fe}}{}_{\mathrm{Tri}}$ and $L^{\mathrm{P}}{}_{\mathrm{Tri}}$ defines the limiting nutrient. We then evaluate dinitrogen fixation as follows:

If iron is limiting :

$$\mu_{\mathrm{FixN_2}} = \mu_{\mathrm{max}}^{\mathrm{Tri}} L_I \frac{\left(\theta^{\mathrm{Fe}} - \theta_0^{\mathrm{Fe}}\right)\theta_{\mathrm{opt}}^{\mathrm{Fe}} - L_{\mathrm{Tri}}^{N}\left(\theta_{\mathrm{opt}}^{\mathrm{Fe}} - \theta_0^{\mathrm{Fe}}\right)\theta^{\mathrm{Fe}}}{\alpha\mu_{\mathrm{max}}^{\mathrm{Tri}}\theta_{\mathrm{opt}}^{\mathrm{Fe}} + \left(\theta_{\mathrm{opt}}^{\mathrm{Fe}} - \theta_0^{\mathrm{Fe}}\right)\theta^{\mathrm{Fe}}}$$

μ_{FixN2} is the growth rate of Trichodesmium sustained by dinitrogen fixation.

else if phosphorus is limiting :

$$\mu_{\mathrm{fixN_2}} = \mu_{\mathrm{max}}^{\mathrm{Tri}} L_I L_P^{\mathrm{Tri}} - \left(\mu_{\mathrm{NO_3}}^{\mathrm{Tri}} + \mu_{\mathrm{NH_4}}^{\mathrm{Tri}}\right)$$

which allows to recalculate the actual iron limitation for *Trichodesmium* as follows

$$L_{\mathrm{Tri}}^{\mathrm{Fe}} = \frac{\left(\theta^{\mathrm{Fe}} - \theta_0^{\mathrm{Fe}} - \alpha\mu_{\mathrm{fixN_2}}\right)\theta_{\mathrm{opt}}^{\mathrm{Fe}}}{\left(\theta_{\mathrm{opt}}^{\mathrm{Fe}} - \theta_0^{\mathrm{Fe}}\right)\theta^{\mathrm{Fe}}}; \alpha = \frac{1}{\beta}$$

β is the marginal use efficiency and equals the moles of additional carbon fixed per additional mole of intracellular iron per day (Raven, 1988; Sunda and Huntsman, 1997).

Such recalculation takes into account the fact that Trichodesmium need much higher cell Fe : C ratios to achieve the same growth rate as if growning on ammonium. That limitation is similar to the previous iron michaelis-menten-type limitation except that the growth rate is zero as long as the Fe : C ratio does not reach 14µmol Fe : mol C (Kustka et al., 2003).

To summarize *Trichodesmium* growth rate:

If $\mu_{FixN_2}=0$: $\mu_{NO_3}^{Tri}=\mu_{max}^{Tri} L_I L_P^{Tri} \frac{L_{NO_3}^{Tri}}{L_{NO_3}^{Tri}+L_{NH_4}^{Tri}}$ and $\mu_{NH_4}^{Tri}=\mu_{max}^{Tri} L_I L_P^{Tri} \frac{L_{NH_4}^{Tri}}{L_{NO_3}^{Tri}+L_{NH_4}^{Tri}}$

If $\mu_{FixN_2}>0$: $\mu_{NO_3}^{Tri}=\mu_{max}^{Tri} L_I L_{NO_3}^{Tri} min(L_P^{Tri}, L_{Fe}^{Tri})$ and $\mu_{NH_4}^{Tri}=\mu_{max}^{Tri} L_I L_{NH_4}^{Tri} min(L_P^{Tri}, L_{Fe}^{Tri})$,

L_P^{Tri} , L_N^{Tri}, L_{Fe}^{Tri} are respectively the *Trichodesmium* limiting function by phosphate, nitrogen and iron. L_I is the *Trichodesmium* limiting function by temperature and light.

μ^{Tri}_{max} is the *Trichodesmium* maximum growth rate,

μ^{Tri}_{NO3} and μ^{Tri}_{NH4} are respectively the new and regenerated productions.

Acknowledgements

We thank the ship captains, the scientists as well as funding agencies of all the projects (OUTPACE, BIOSOPE, MOORSPICE, DIAPALIS , NECTALIS, PANDORA, Mirai) that allowed data collection without which we could not validate our model. The authors thank Institute of Research for Development for supporting all authors. Cyril Dutheil is funded by European project INTEGRE.

References

Arrigo, K. R.: Marine microorganisms and global nutrient cycles, Nature, 437(7057), 349–355, doi:10.1038/nature04159, 2005.

Aumont, O. and Bopp, L.: Globalizing results from ocean in situ iron fertilization studies: globalizing iron fertilization, Glob. Biogeochem. Cycles, 20(2), n/a-n/a, doi:10.1029/2005GB002591, 2006b.

Aumont, O., Ethé, C., Tagliabue, A., Bopp, L. and Gehlen, M.: PISCES-v2: an ocean biogeochemical model for carbon and ecosystem studies, Geosci. Model Dev. Discuss., 8(2), 1375–1509, doi:10.5194/gmdd-8-1375-2015, 2015.

Bennett, S. A., Achterberg, E. P., Connelly, D. P., Statham, P. J., Fones, G. R. and German, C. R.: The distribution and stabilisation of dissolved Fe in deep-sea hydrothermal plumes, Earth Planet. Sci. Lett., 270(3–4), 157–167, doi:10.1016/j.epsl.2008.01.048, 2008.

Bergman, B., Sandh, G., Lin, S., Larsson, J. and Carpenter, E. J.: Trichodesmium – a widespread marine

cyanobacterium with unusual nitrogen fixation properties, FEMS Microbiol. Rev., 37(3), 286–302, doi:10.1111/j.1574-6976.2012.00352.x, 2013.

Berman-Frank, I.: Segregation of Nitrogen Fixation and Oxygenic Photosynthesis in the Marine Cyanobacterium Trichodesmium, Science, 294(5546), 1534–1537, doi:10.1126/science.1064082, 2001.

Berthelot, H., Bonnet, S., Camps, M., Grosso, O. and Moutin, T.: Assessment of the dinitrogen released as ammonium and dissolved organic nitrogen by unicellular and filamentous marine diazotrophic cyanobacteria grown in culture, Front. Mar. Sci., 2, doi:10.3389/fmars.2015.00080, 2015.

Berthelot, H., Bonnet, S., Grosso, O., Cornet, V. and Barani, A.: Transfer of diazotroph-derived nitrogen towards non-diazotrophic planktonic communities: a comparative study between Trichodesmium erythraeum, Crocosphaera watsonii and Cyanothece sp., Biogeosciences, 13(13), 4005–4021, doi:10.5194/bg-13-4005-2016, 2016.

Berthelot, H., Benavides, M., Moisander, P. H., Grosso, O. and Bonnet, S.: High-nitrogen fixation rates in the particulate and dissolved pools in the Western Tropical Pacific (Solomon and Bismarck Seas): N 2 Fixation in the Western Pacific, Geophys. Res. Lett., 44(16), 8414–8423, doi:10.1002/2017GL073856, 2017.

Bissett, W. P., Walsh, J. J., Dieterle, D. A. and Carder, K. L.: Carbon cycling in the upper waters of the Sargasso Sea: I. Numerical simulation of differential carbon and nitrogen fluxes, Deep Sea Res. Part Oceanogr. Res. Pap., 46(2), 205–269, doi:10.1016/S0967-0637(98)00062-4, 1999.

Bombar, D., Paerl, R. W. and Riemann, L.: Marine Non-Cyanobacterial Diazotrophs: Moving beyond Molecular Detection, Trends Microbiol., 24(11), 916–927, doi:10.1016/j.tim.2016.07.002, 2016.

Bonnet, S., Biegala, I. C., Dutrieux, P., Slemons, L. O. and Capone, D. G.: Nitrogen fixation in the western equatorial Pacific: Rates, diazotrophic cyanobacterial size class distribution, and biogeochemical significance: N 2 fixation in the equatorial pacific, Glob. Biogeochem. Cycles, 23(3), n/a-n/a, doi:10.1029/2008GB003439, 2009.

Bonnet, S., Rodier, M., Turk-Kubo, K. A., Germineaud, C., Menkes, C., Ganachaud, A., Cravatte, S., Raimbault, P., Campbell, E., Quéroué, F., Sarthou, G., Desnues, A., Maes, C. and Eldin, G.: Contrasted geographical distribution of N 2 fixation rates and nif H phylotypes in the Coral and Solomon Seas (southwestern Pacific) during austral winter conditions: N 2 fixation and diversity in the pacific, Glob. Biogeochem. Cycles, 29(11), 1874–1892, doi:10.1002/2015GB005117, 2015b.

Bonnet, S., Berthelot, H., Turk-Kubo, K., Cornet-Barthaux, V., Fawcett, S., Berman-Frank, I., Barani, A., Grégori, G., Dekaezemacker, J., Benavides, M. and Capone, D. G.: Diazotroph derived nitrogen supports diatom growth in the South West Pacific: A quantitative study using nanoSIMS: Transfer of diazotrophic N into plankton, Limnol. Oceanogr., 61(5), 1549–1562, doi:10.1002/lno.10300, 2016a.

Bonnet, S., Berthelot, H., Turk-Kubo, K., Fawcett, S., Rahav, E., L'Helguen, S. and Berman-Frank, I.: Dynamics of N2 fixation and fate of diazotroph-derived nitrogen in a low-nutrient, low-chlorophyll ecosystem: results from the VAHINE mesocosm experiment (New Caledonia), Biogeosciences, 13(9), 2653–2673, doi:10.5194/bg-13-2653-2016, 2016b.

Bonnet, S., Caffin, M., Berthelot, H. and Moutin, T.: Hot spot of N2 fixation in the western tropical South Pacific pleads for a spatial decoupling between N2 fixation and denitrification, Proc. Natl. Acad. Sci., 114(14), E2800–E2801, 2017.

Böttjer, D., Dore, J. E., Karl, D. M., Letelier, R. M., Mahaffey, C., Wilson, S. T., Zehr, J. and Church, M. J.: Temporal variability of nitrogen fixation and particulate nitrogen export at Station ALOHA: Temporal variability of nitrogen fixation and particulate nitrogen, Limnol. Oceanogr., 62(1), 200–216, doi:10.1002/lno.10386, 2017.

Breitbarth, E., Wohlers, J., Kläs, J., LaRoche, J. and Peeken, I.: Nitrogen fixation and growth rates of Trichodesmium IMS-101 as a function of light intensity, Mar. Ecol. Prog. Ser., 359, 25–36, doi:10.3354/meps07241, 2008.

Capone, D. G.: Trichodesmium, a Globally Significant Marine Cyanobacterium, Science, 276(5316), 1221–1229, doi:10.1126/science.276.5316.1221, 1997.

Carpenter, E. J.: Nitrogen Fixation by a Blue-Green Epiphyte on Pelagic Sargassum, Science, 178(4066), 1207–1209, doi:10.1126/science.178.4066.1207, 1972.

Church, M. J., Jenkins, B. D., Karl, D. M. and Zehr, J. P.: Vertical distributions of nitrogen-fixing phylotypes at Stn ALOHA in the oligotrophic North Pacific Ocean, Aquat. Microb. Ecol., 38(1), 3–14, 2005.

Codispoti, L. A., Brandes, J. A., Christensen, J. P., Devol, A. H., Naqvi, S. W. A., Paerl, H. W. and Yoshinari, T.: The oceanic fixed nitrogen and nitrous oxide budgets: Moving targets as we enter the anthropocene?, Sci. Mar., 65(S2), 85–105, doi:10.3989/scimar.2001.65s285, 2001.

Couvelard, X., Marchesiello, P., Gourdeau, L. and Lefèvre, J.: Barotropic Zonal Jets Induced by Islands in the Southwest Pacific, J. Phys. Oceanogr., 38(10), 2185–2204, doi:10.1175/2008JPO3903.1, 2008.

Cravatte, S., Madec, G., Izumo, T., Menkes, C. and Bozec, A.: Progress in the 3-D circulation of the eastern equatorial Pacific in a climate ocean model, Ocean Model., 17(1), 28–48, doi:10.1016/j.ocemod.2006.11.003, 2007.

Delmont, T. O., Quince, C., Shaiber, A., Esen, O. C., Lee, S. T. M., Lucker, S. and Eren, A. M.: Nitrogen-Fixing Populations Of Planctomycetes And Proteobacteria Are Abundant In The Surface Ocean, , doi:10.1101/129791, 2017.

Deutsch, C., Gruber, N., Key, R. M., Sarmiento, J. L. and Ganachaud, A.: Denitrification and N 2 fixation in the Pacific Ocean, Glob. Biogeochem. Cycles, 15(2), 483–506, doi:10.1029/2000GB001291, 2001.

Deutsch, C., Sarmiento, J. L., Sigman, D. M., Gruber, N. and Dunne, J. P.: Spatial coupling of nitrogen inputs and losses in the ocean, Nature, 445(7124), 163–167, doi:10.1038/nature05392, 2007.

Droop, M. R.: 25 Years of Algal Growth Kinetics A Personal View, Bot. Mar., 26(3), doi:10.1515/botm.1983.26.3.99, 1983.

Dupouy, C., Neveux, J., Subramaniam, A., Mulholland, M. R., Montoya, J. P., Campbell, L., Carpenter, E. J. and Capone, D. G.: Satellite captures trichodesmium blooms in the southwestern tropical Pacific, Eos Trans. Am. Geophys. Union, 81(2), 13, doi:10.1029/00EO00008, 2000.

Dupouy, C., Benielli-Gary, D., Neveux, J., Dandonneau, Y. and Westberry, T. K.: An algorithm for detecting Trichodesmium surface blooms in the South Western Tropical Pacific, Biogeosciences, 8, 3631–3647, 2011.

Dutkiewicz, S., Ward, B. A., Monteiro, F. and Follows, M. J.: Interconnection of nitrogen fixers and iron in the Pacific Ocean: Theory and numerical simulations: marine nitrogen fixers and iron, Glob. Biogeochem. Cycles, 26(1), n/a-n/a, doi:10.1029/2011GB004039, 2012.

Falcón, L. I., Pluvinage, S. and Carpenter, E. J.: Growth kinetics of marine unicellular N2-fixing cyanobacterial isolates in continuous culture in relation to phosphorus and temperature, Mar. Ecol. Prog. Ser., 285, 3–9, 2005.

Fennel, K., Spitz, Y. H., Letelier, R. M., Abbott, M. R. and Karl, D. M.: A deterministic model for N 2 fixation at stn. ALOHA in the subtropical North Pacific Ocean, Deep Sea Res. Part II Top. Stud. Oceanogr., 49(1), 149–174, 2001.

Gallon, J. R.: Reconciling the incompatible: N2 fixation And O2, New Phytol., 122(4), 571–609, doi:10.1111/j.1469-8137.1992.tb00087.x, 1992.

Galloway, J. N., Dentener, F. J., Capone, D. G., Boyer, E. W., Howarth, R. W., Seitzinger, S. P., Asner, G. P., Cleveland, C. C., Green, P. A., Holland, E. A., Karl, D. M., Michaels, A. F., Porter, J. H., Townsend, A. R. and Vörösmarty, C. J.: Nitrogen Cycles: Past, Present, and Future, Biogeochemistry, 70(2), 153–226, doi:10.1007/s10533-004-0370-0, 2004.

Garcia, N., Raimbault, P. and Sandroni, V.: Seasonal nitrogen fixation and primary production in the Southwest Pacific: nanoplankton diazotrophy and transfer of nitrogen to picoplankton organisms, Mar. Ecol. Prog. Ser., 343, 25–33, doi:10.3354/meps06882, 2007.

Goebel, N. L., Edwards, C. A., Carter, B. J., Achilles, K. M. and Zehr, J. P.: Growth and carbon content of three different-sized diazotrophic cyanobacteria observed in the subtropical north pacific, J. Phycol., 44(5), 1212–1220, doi:10.1111/j.1529-8817.2008.00581.x, 2008.

Großkopf, T., Mohr, W., Baustian, T., Schunck, H., Gill, D., Kuypers, M. M. M., Lavik, G., Schmitz, R. A., Wallace, D. W. R. and LaRoche, J.: Doubling of marine dinitrogen-fixation rates based on direct measurements, Nature, 488(7411), 361–364, doi:10.1038/nature11338, 2012.

Gruber, N.: Oceanography: A bigger nitrogen fix, Nature, 436(7052), 786–787, 2005.

Gruber, N.: The Marine Nitrogen Cycle: Overview and challenges, in Nitrogen in the Marine Environment, pp. 1–50, Elsevier., 2008.

Halm, H., Lam, P., Ferdelman, T. G., Lavik, G., Dittmar, T., LaRoche, J., D'Hondt, S. and Kuypers, M. M.: Heterotrophic organisms dominate nitrogen fixation in the South Pacific Gyre, ISME J., 6(6), 1238–1249, doi:10.1038/ismej.2011.182, 2012.

Hood, R. R., Bates, N. R., Capone, D. G. and Olson, D. B.: Modeling the effect of nitrogen fixation on carbon and nitrogen fluxes at BATS, Deep Sea Res. Part II Top. Stud. Oceanogr., 48(8–9), 1609–1648, doi:10.1016/S0967-0645(00)00160-0, 2001.

Johnson, K. S., Chavez, F. P. and Friederich, G. E.: Continental-shelf sediment as a primary source of iron for coastal phytoplankton, Nature, 398(6729), 697–700, doi:10.1038/19511, 1999.

Jullien, S., Menkes, C. E., Marchesiello, P., Jourdain, N. C., Lengaigne, M., Koch-Larrouy, A., Lefèvre, J., Vincent, E. M. and Faure, V.: Impact of Tropical Cyclones on the Heat Budget of the South Pacific Ocean, J. Phys. Oceanogr., 42(11), 1882–1906, doi:10.1175/JPO-D-11-0133.1, 2012.

Jullien, S., Marchesiello, P., Menkes, C. E., Lef?vre, J., Jourdain, N. C., Samson, G. and Lengaigne, M.: Ocean feedback to tropical cyclones: climatology and processes, Clim. Dyn., 43(9–10), 2831–2854, doi:10.1007/s00382-014-2096-6, 2014.

Karl, D., Letelier, R., Tupas, L., Dore, J., Christian, J. and Hebel, D.: The role of nitrogen fixation in biogeochemical cycling in the subtropical North Pacific Ocean, Nature, 388(6642), 533–538, 1997.

Keith Moore, J., Doney, S. C., Lindsay, K., Mahowald, N. and Michaels, A. F.: Nitrogen fixation amplifies the ocean biogeochemical response to decadal timescale variations in mineral dust deposition, Tellus B Chem. Phys. Meteorol., 58(5), 560–572, doi:10.1111/j.1600-0889.2006.00209.x, 2006.

Krishnamurthy, A., Moore, J. K., Mahowald, N., Luo, C., Doney, S. C., Lindsay, K. and Zender, C. S.: Impacts of increasing anthropogenic soluble iron and nitrogen deposition on ocean biogeochemistry: atmospheric Fe and N and ocean biogoechemistry, Glob. Biogeochem. Cycles, 23(3), n/a-n/a, doi:10.1029/2008GB003440, 2009.

Kromkamp, J. and Walsby, A. E.: Buoyancy Regulation and Vertical Migration of Trichodesmium: a Computer-Model Prediction, in Marine Pelagic Cyanobacteria: Trichodesmium and other Diazotrophs, edited by E. J. Carpenter, D. G. Capone, and J. G. Rueter, pp. 239–248, Springer Netherlands, Dordrecht., 1992.

Küpper, H., etlk, I., Seibert, S., Pril, O., etlikova, E., Strittmatter, M., Levitan, O., Lohscheider, J., Adamska, I. and Berman-Frank, I.: Iron limitation in the marine cyanobacterium Trichodesmium reveals new insights into regulation of photosynthesis and nitrogen fixation, New Phytol., 179(3), 784–798, doi:10.1111/j.1469-8137.2008.02497.x, 2008.

Kustka, A. B., Sanudo-Wilhelmy, S. A., Carpenter, E. J., Capone, D., Burns, J. and Sunda, W. G.: Iron requirements for dinitrogen-and ammonium-supported growth in cultures of Trichodesmium (IMS 101): Comparison with nitrogen fixation rates and iron: carbon ratios of field populations, Limnol. Oceanogr., 48(5), 1869–1884, 2003.

Large, W. G., McWilliams, J. C. and Doney, S. C.: Oceanic vertical mixing: A review and a model with a nonlocal

boundary layer parameterization, Rev. Geophys., 32(4), 363, doi:10.1029/94RG01872, 1994.
LaRoche, J. and Breitbarth, E.: Importance of the diazotrophs as a source of new nitrogen in the ocean, J. Sea Res., 53(1–2), 67–91, doi:10.1016/j.seares.2004.05.005, 2005.
Letelier, R. and Karl, D.: Trichodesmium spp. physiology and nutrient fluxes in the North Pacific subtropical gyre, Aquat. Microb. Ecol., 15, 265–276, doi:10.3354/ame015265, 1998.
Luo, Y.-W., Doney, S. C., Anderson, L. A., Benavides, M., Berman-Frank, I., Bode, A., Bonnet, S., Boström, K. H., Böttjer, D., Capone, D. G., Carpenter, E. J., Chen, Y. L., Church, M. J., Dore, J. E., Falcón, L. I., Fernández, A., Foster, R. A., Furuya, K., Gómez, F., Gundersen, K., Hynes, A. M., Karl, D. M., Kitajima, S., Langlois, R. J., LaRoche, J., Letelier, R. M., Marañón, E., McGillicuddy, D. J., Moisander, P. H., Moore, C. M., Mouriño-Carballido, B., Mulholland, M. R., Needoba, J. A., Orcutt, K. M., Poulton, A. J., Rahav, E., Raimbault, P., Rees, A. P., Riemann, L., Shiozaki, T., Subramaniam, A., Tyrrell, T., Turk-Kubo, K. A., Varela, M., Villareal, T. A., Webb, E. A., White, A. E., Wu, J. and Zehr, J. P.: Database of diazotrophs in global ocean: abundance, biomass and nitrogen fixation rates, Earth Syst. Sci. Data, 4(1), 47–73, doi:10.5194/essd-4-47-2012, 2012.
Luo, Y.-W., Lima, I. D., Karl, D. M., Deutsch, C. A. and Doney, S. C.: Data-based assessment of environmental controls on global marine nitrogen fixation, Biogeosciences, 11(3), 691–708, doi:10.5194/bg-11-691-2014, 2014.
Marchesiello, P., McWilliams, J. C. and Shchepetkin, A.: Open boundary conditions for long-term integration of regional oceanic models, Ocean Model., 3(1–2), 1–20, doi:10.1016/S1463-5003(00)00013-5, 2001.
Marchesiello, P., Lefèvre, J., Vega, A., Couvelard, X. and Menkes, C.: Coastal upwelling, circulation and heat balance around New Caledonia's barrier reef, Mar. Pollut. Bull., 61(7–12), 432–448, doi:10.1016/j.marpolbul.2010.06.043, 2010.
Mills, M. M., Ridame, C., Davey, M., La Roche, J. and Geider, R. J.: Iron and phosphorus co-limit nitrogen fixation in the eastern tropical North Atlantic, Nature, 429(6989), 292–294, 2004.
Mohr, W., Großkopf, T., Wallace, D. W. R. and LaRoche, J.: Methodological Underestimation of Oceanic Nitrogen Fixation Rates, edited by Z. Finkel, PLoS ONE, 5(9), e12583, doi:10.1371/journal.pone.0012583, 2010.
Moisander, P. H., Beinart, R. A., Voss, M. and Zehr, J. P.: Diversity and abundance of diazotrophic microorganisms in the South China Sea during intermonsoon, ISME J., 2(9), 954–967, 2008.
Moisander, P. H., Beinart, R. A., Hewson, I., White, A. E., Johnson, K. S., Carlson, C. A., Montoya, J. P. and Zehr, J. P.: Unicellular cyanobacterial distributions broaden the oceanic N2 fixation domain, Science, 327(5972), 1512–1514, 2010.
Moisander, P. H., Benavides, M., Bonnet, S., Berman-Frank, I., White, A. E. and Riemann, L.: Chasing after Non-cyanobacterial Nitrogen Fixation in Marine Pelagic Environments, Front. Microbiol., 8, doi:10.3389/fmicb.2017.01736, 2017.
Monod, J.: Recherches sur la croissance des cultures bactériennes., Hermann & cie, Paris., 1942.
Monteiro, F. M., Dutkiewicz, S. and Follows, M. J.: Biogeographical controls on the marine nitrogen fixers: controls on marine nitrogen fixers, Glob. Biogeochem. Cycles, 25(2), n/a-n/a, doi:10.1029/2010GB003902, 2011.
Montoya, J. P., Holl, C. M., Zehr, J. P., Hansen, A., Villareal, T. A. and Capone, D. G.: High rates of N2 fixation by unicellular diazotrophs in the oligotrophic Pacific Ocean, Nature, 430(7003), 1027–1032, doi:10.1038/nature02824, 2004.
Moore, C. M., Mills, M. M., Arrigo, K. R., Berman-Frank, I., Bopp, L., Boyd, P. W., Galbraith, E. D., Geider, R. J., Guieu, C., Jaccard, S. L., Jickells, T. D., La Roche, J., Lenton, T. M., Mahowald, N. M., Marañón, E., Marinov, I., Moore, J. K., Nakatsuka, T., Oschlies, A., Saito, M. A., Thingstad, T. F., Tsuda, A. and Ulloa, O.: Processes and patterns of oceanic nutrient limitation, Nat. Geosci., 6(9), 701–710, doi:10.1038/ngeo1765, 2013.

Moore, J. K., Doney, S. C., Kleypas, J. A., Glover, D. M. and Fung, I. Y.: An intermediate complexity marine ecosystem model for the global domain, Deep Sea Res. Part II Top. Stud. Oceanogr., 49(1), 403–462, 2001.

Moore, J. K., Doney, S. C. and Lindsay, K.: Upper ocean ecosystem dynamics and iron cycling in a global three-dimensional model: global ecosystem-biogeochemical model, Glob. Biogeochem. Cycles, 18(4), n/a-n/a, doi:10.1029/2004GB002220, 2004.

Moutin, T., Van Den Broeck, N., Beker, B., Dupouy, C., Rimmelin, P. and Le Bouteiller, A.: Phosphate availability controls Trichodesmium spp. biomass in the SW Pacific Ocean, Mar. Ecol. Prog. Ser., 297(1), 15–21, 2005.

Moutin, T., Karl, D. M., Duhamel, S., Rimmelin, P., Raimbault, P., Van Mooy, B. A. S. and Claustre, H.: Phosphate availability and the ultimate control of new nitrogen input by nitrogen fixation in the tropical Pacific Ocean, Biogeosciences, 5(1), 95–109, doi:10.5194/bg-5-95-2008, 2008.

Mulholland, M. R. and Capone, D. G.: The nitrogen physiology of the marine N2-fixing cyanobacteria Trichodesmium spp., Trends Plant Sci., 5(4), 148–153, doi:10.1016/S1360-1385(00)01576-4, 2000.

Mulholland, M. R., Ohki, K. and Capone, D. G.: Nutrient controls on nitrogen uptake and metabolism by natural populations and cultures of Trichodesmium (cyanobacteria), J. Phycol., 37(6), 1001–1009, doi:10.1046/j.1529-8817.2001.00080.x, 2001.

Neveux, J., Tenírio, M. M. B., Dupouy, Cé. and Villareal, T. A.: Spectral diversity of phycoerythrins and diazotroph abundance in tropical waters, Limnol. Oceanogr., 51(4), 1689–1698, doi:10.4319/lo.2006.51.4.1689, 2006.

Ohki, K., Zehr, J. P. and Fujita, Y.: Regulation of nitrogenase activity in relation to the light-dark regime in the filamentous non-heterocystous cyanobacterium Trichodesmium sp. NIBB 1067, Microbiology, 138(12), 2679–2685, 1992.

Paerl, H. W., Priscu, J. C. and Brawner, D. L.: Immunochemical localization of nitrogenase in marine Trichodesmium aggregates: Relationship to N2 fixation potential, Appl. Environ. Microbiol., 55(11), 2965–2975, 1989.

Penven, P., Debreu, L., Marchesiello, P. and McWilliams, J. C.: Evaluation and application of the ROMS 1-way embedding procedure to the central california upwelling system, Ocean Model., 12(1–2), 157–187, doi:10.1016/j.ocemod.2005.05.002, 2006.

Postgate, J. R.: Biology nitrogen fixation: fundamentals, Philos. Trans. R. Soc. Lond. B Biol. Sci., 296(1082), 375–385, 1982.

Radic, A., Lacan, F. and Murray, J. W.: Iron isotopes in the seawater of the equatorial Pacific Ocean: New constraints for the oceanic iron cycle, Earth Planet. Sci. Lett., 306(1–2), 1–10, doi:10.1016/j.epsl.2011.03.015, 2011.

Raimbault, P. and Garcia, N.: Evidence for efficient regenerated production and dinitrogen fixation in nitrogen-deficient waters of the South Pacific Ocean: impact on new and export production estimates, Biogeosciences, 5(2), 323–338, 2008.

Ramamurthy, V. D. and Krishnamurthy, S.: Effects of N: P ratios on the uptake of nitrate and phosphate by laboratory cultures ofTrichodesmium erythraeum (Ehr.), Proc. Plant Sci., 65(2), 43–48, 1967.

Raven, J. A.: The iron and molybdenum use efficiencies of plant growth with different energy, carbon and nitrogen sources, New Phytol., 109(3), 279–287, doi:10.1111/j.1469-8137.1988.tb04196.x, 1988.

Rubin, M., Berman-Frank, I. and Shaked, Y.: Dust- and mineral-iron utilization by the marine dinitrogen-fixer Trichodesmium, Nat. Geosci., 4(8), 529–534, doi:10.1038/ngeo1181, 2011.

Rueter, J. G.: Iron stimulation of photosynthesis and nitrogen fixation in Anabaena 7120 and Trichodesmium (Cyanophyceae), J. Phycol., 24(2), 249–254, doi:10.1111/j.1529-8817.1988.tb04240.x, 1988.

Shchepetkin, A. F. and McWilliams, J. C.: Quasi-Monotone Advection Schemes Based on Explicit Locally Adaptive

Dissipation, Mon. Weather Rev., 126(6), 1541–1580, doi:10.1175/1520-0493(1998)126<1541:QMASBO>2.0.CO;2, 1998.

Shchepetkin, A. F. and McWilliams, J. C.: The regional oceanic modeling system (ROMS): a split-explicit, free-surface, topography-following-coordinate oceanic model, Ocean Model., 9(4), 347–404, doi:10.1016/j.ocemod.2004.08.002, 2005.

Shiozaki, T., Kodama, T., Kitajima, S., Sato, M. and Furuya, K.: Advective transport of diazotrophs and importance of their nitrogen fixation on new and primary production in the western Pacific warm pool, Limnol. Oceanogr., 58(1), 49–60, doi:10.4319/lo.2013.58.1.0049, 2013.

Shiozaki, T., Kodama, T. and Furuya, K.: Large-scale impact of the island mass effect through nitrogen fixation in the western South Pacific Ocean: island mass effect through N2 fixation, Geophys. Res. Lett., 41(8), 2907–2913, doi:10.1002/2014GL059835, 2014.

Shiozaki, T., Nagata, T., Ijichi, M. and Furuya, K.: Nitrogen fixation and the diazotroph community in the temperate coastal region of the northwestern North Pacific, Biogeosciences, 12(15), 4751–4764, doi:10.5194/bg-12-4751-2015, 2015.

Staal, M., Filip, Meysman and Lucas: Temperature excludes N2-fixing heterocystous cyanobacteria in the tropical oceans, Nature, 425(6957), 501–504, doi:10.1038/nature02001, 2003.

Sunda, W. G. and Huntsman, S. A.: Interrelated influence of iron, light and cell size on marine phytoplankton growth, Nature, 390(6658), 389–392, doi:10.1038/37093, 1997.

Tagliabue, A., Bopp, L. and Aumont, O.: Ocean biogeochemistry exhibits contrasting responses to a large scale reduction in dust deposition, Biogeosciences, 5(1), 11–24, 2008.

Tagliabue, A., Bopp, L., Dutay, J.-C., Bowie, A. R., Chever, F., Jean-Baptiste, P., Bucciarelli, E., Lannuzel, D., Remenyi, T., Sarthou, G., Aumont, O., Gehlen, M. and Jeandel, C.: Hydrothermal contribution to the oceanic dissolved iron inventory, Nat. Geosci., 3(4), 252–256, doi:10.1038/ngeo818, 2010.

Tagliabue, A., Mtshali, T., Aumont, O., Bowie, A. R., Klunder, M. B., Roychoudhury, A. N. and Swart, S.: A global compilation of dissolved iron measurements: focus on distributions and processes in the Southern Ocean, Biogeosciences, 9(6), 2333–2349, doi:10.5194/bg-9-2333-2012, 2012.

Toner, B. M., Fakra, S. C., Manganini, S. J., Santelli, C. M., Marcus, M. A., Moffett, J. W., Rouxel, O., German, C. R. and Edwards, K. J.: Preservation of iron(II) by carbon-rich matrices in a hydrothermal plume, Nat. Geosci., 2(3), 197–201, doi:10.1038/ngeo433, 2009.

Turk-Kubo, K. A., Karamchandani, M., Capone, D. G. and Zehr, J. P.: The paradox of marine heterotrophic nitrogen fixation: abundances of heterotrophic diazotrophs do not account for nitrogen fixation rates in the Eastern Tropical South Pacific: N 2 -fixing potential of heterotrophs in the ETSP, Environ. Microbiol., 16(10), 3095–3114, doi:10.1111/1462-2920.12346, 2014.

Villareal, T. A. and Carpenter, E. J.: Diel buoyancy regulation in the marine diazotrophic cyanobacterium Trichodesmium thiebautii, Limnol. Oceanogr., 35(8), 1832–1837, doi:10.4319/lo.1990.35.8.1832, 1990.

Villareal, T. A. and Carpenter, E. J.: Buoyancy Regulation and the Potential for Vertical Migration in the Oceanic Cyanobacterium Trichodesmium, Microb. Ecol., 45(1), 1–10, doi:10.1007/s00248-002-1012-5, 2003.

White, A., Spitz, Y. and Letelier, R.: Modeling carbohydrate ballasting by Trichodesmium spp., Mar. Ecol. Prog. Ser., 323, 35–45, doi:10.3354/meps323035, 2006.

Ye, Y., Völker, C., Bracher, A., Taylor, B. and Wolf-Gladrow, D. A.: Environmental controls on N2 fixation by Trichodesmium in the tropical eastern North Atlantic Ocean—A model-based study, Deep Sea Res. Part Oceanogr. Res.

Pap., 64, 104–117, doi:10.1016/j.dsr.2012.01.004, 2012.

Zehr, J. P. and Bombar, D.: Marine Nitrogen Fixation: Organisms, Significance, Enigmas, and Future Directions, in Biological Nitrogen Fixation, edited by F. J. de Bruijn, pp. 855–872, John Wiley & Sons, Inc, Hoboken, NJ, USA., 2015.

Table 1 : Models parameters for Trichodemium and nanophytoplakton.

Parameters	Symbol	Name in code	Unity	Value
Initial slope P-I tricho	αI	pislope1	$(W.m^{-2})^{-1}\ d^{-1}$	0.072
Initial slope P-I nano	αI	pislope	$(W\ m^{-2})^{-1}\ d^{-1}$	2.0
Microzoo preference for tricho	pItri	xpref2t	-	0.5
Microzoo preference for nano	pIP	xpref2p	-	1.0
Mesozoo preference for tricho	pItri	xpreft	-	0.3
Mesozoo preference for nano	pIP	xprefp	-	0.3
Tricho feeding threshold for mesozoo	Tithresh	xthresh2tri	$mol\ C\ L^{-1}$	1.10^{-8}
Nanophyto feeding threshold for mesozoo	Pithresh	xthresh2phy	$mol\ C\ L^{-1}$	1.10^{-8}
Tricho feeding threshold for microzoo	Tithresh	xthreshtri	$mol\ C\ L^{-1}$	1.10^{-8}
Nanophyto feeding threshold for microzoo	Pithresh	xthreshphy	$mol\ C\ L^{-1}$	1.10^{-8}
NO3 half saturation of tricho	KTriNO3	conctno3	$mol\ N\ L^{-1}$	1.10^{-6}
NO3 half saturation of nanophyto	KPNO3	concnno3	$mol\ N\ L^{-1}$	1.10^{-6}
NH4 half saturation of tricho	KTriNH4	conctnh4	$mol\ N\ L^{-1}$	5.10^{-7}
NH4 half saturation of nanophyto	KPNH4	concnnh4	$mol\ N\ L^{-1}$	5.10^{-7}
PO4 half saturation of tricho	KTriPO4	conctpo4	$mol\ P\ L^{-1}$	5.10^{-6}
PO4 half saturation of nanophyto	KPPO4	concnpo4	$mol\ P\ L^{-1}$	5.10^{-6}
Iron half saturation for tricho	KtriFe	conctfer	$mol\ Fe\ L^{-1}$	1.10^{-9}
Iron half saturation for nanophyto	KPFe	concnfer	$mol\ Fe\ L^{-1}$	1.10^{-9}
Minimum size criteria for tricho	Imax	xsizetri	$mol\ C\ L^{-1}$	1.10^{-6}
Minimum size criteria for nanophyto	Imax	xsizephy	$mol\ C\ L^{-1}$	1.10^{-6}
Optimal Fe quota for tricho	θFe,Triopt	qtfelim	$mol\ Fe\ (mol\ C)^{-1}$	7.10^{-6}
Optimal Fe quota for nanophyto	θFe,Iopt	qnfelim	$mol\ Fe\ (mol\ C)^{-1}$	7.10^{-6}
Minimum Chl/C in tricho	θChl,Trimin	chlctm	$mg\ Chl\ (mg\ C)^{-1}$	0.033
Minimum Chl/C in nanophyto	θChl,Imin	chlcnm	$mg\ Chl\ (mg\ C)^{-1}$	0.033
Maximum Fe/C in tricho	θFe,Trimax	fectm	$mol\ Fe\ (mol\ C)^{-1}$	1.10^{-4}
Maximum Fe/C in nanophyto	θFe,Imax	fecnm	$mol\ Fe\ (mol\ C)^{-1}$	4.10^{-5}
Maximum N/C in tricho	θN,Trimax	qntlm	$mol\ N\ (mol\ C)^{-1}$	1.45
Maximum N/C in nanophyto	θN,Imax	qnnlm	mol N (mol C)-1	1.45
Maximum P/C in tricho	θP,Trimax	qptlm	$mol\ P\ (mol\ C)^{-1}$	2.44
Maximum P/C in nanophyto	θN,Imax	qpnlm	$mol\ P\ .(mol\ C)^{-1}$	2.44
Excretion ratio of tricho	rTri	excret1	d^{-1}	0.05
Excretion ratio of nanophyto	rI	excret	d^{-1}	0.05
Maintenance iron	m	zfixbasal	$mol\ Fe\ .(mol\ C)^{-1}$	$1.4.10^{-5}$
Marginal use efficiency	β	qfec	day^{-1}	$1.4.10^{-4}$

Table 2 : List and description of the different experiments.

Name configuration	N_2 fixation	Iron from sediment
TRI	explicit	yes
TRI_NoFeSed	explicit	no
N2_imp	implicit	yes
Wo_N2	no	yes

790 **Figures caption**

Fig. 1 : Annual mean concentrations in µmol L^{-1}: a) PO4 data from the CARS b) PO4 simulated by ROMS-PISCES model c) NO3 data from the CARS d) NO3 simulated by ROMS-PISCES model. On panels a and b the black contours show the annual mean of patterns of temperature prefenrendum from observations (a) and model (b). The red contours displays the 26°C isolign for austral winter (plain) and austral summer (dash). On panels (c) and (d) the red boxes represent the LNLC regions.

Fig. 2 : Left : Boxplots of the 0-150 averaged Iron (nmol $Fe.L^{-1}$) data (blue) and the equivalent for the model (red) colocalised with the observations in space. The coloured box represents the 25-75% of the distribution, the whiskers the 10-90% distribution. The line into the coloured box is the median.

Right : Iron concentrations (nmol $Fe.L^{-1}$) as observed (b) and as simulated by the model (c). Iron concentrations has been averaged over the top 150m of the ocean. Model values have been sampled at the same location, the same month, and the same depth as the data.

Fig. 3 : Top : Annual mean Chlorophyll concentration (in mg $Chl.m^{-3}$) in surface from (a) GLOBCOLOUR data (b) TRI simulation (c) TRI_imp simulation.

Bottom (d) : Annual mean Trichodesmium chlorophyll (in mg $Chl.m^{-3}$) in surface from TRI simulation

Fig. 4 : Nitrogen fixation rates (µmol $N.m^{-2}d^{-1}$) as observed (left) and as simulated by TRI simulation (right).

Top : Nitrogen fixation rates has been integrated over the top 150m of the ocean.

Bottom : Nitrogen fixation rates has been averaged over the top 30m of the ocean.

Model values have been sampled at the same location, the same month, and the same depth as the data.

Fig. 5 : a) Depth-integrated (0 to 125m) rates of nitrogen fixation (µmol $N.m^{-2}d^{-1}$) at ALOHA for the data (blue) and TRI simulation (red).

b) Depth-integrated (0 to 150m) rates of nitrogen fixation (µmol $N.m^{-2}d^{-1}$) in the south pacific (red box, Fig. 1c) for the data (blue) and TRI simulation (red). The green curve is the averaged of the seasonal cycle from TRI simulation at the data positions. Model values have been sampled at the same location, the same month, and the same depth as the data.

Fig. 6 : Relative contribution (in percentage) of *Trichodesmium* to primary production.

Fig. 7 : *Trichodesmium* biomass (mmol $C.m^{-2}$) for a) austral summer and b) austral winter, integrated over the top 100m of the ocean.

Fig. 8 : Seasonal cycle of limitation terms for *Trichodesmium* production in a) South Pacific and b) North Pacific. The right scale represents the total limitation.

Fig. 9 : Top : Minimum, mean and maximum in the South box (Fig 1c) for (a) iron concentration, (b) chlorophyll concentration in Trichodesmium.

Bottom : Annual mean iron concentration (shading ; in nmol $Fe.L^{-1}$) and current (vectors ; in $m.s^{-1}$) for c) TRI_NoFeSed simulation and d) TRI simulation. Annual mean Chlorophyll concentration in *Trichodesmium* (mg $Chl.m^{-3}$) for e) TRI_NoFeSed simulation and f) TRI simulation. The concentrations have been averaged over the top 100m of the ocean.

Fig. 10 : Percentage increase of primary production between the TRI simulation and Wo_N2 simulation (top) and N2_imp simulation (bottom); for total primary production (left) and primary production from Nanophyto. + diatoms (right).

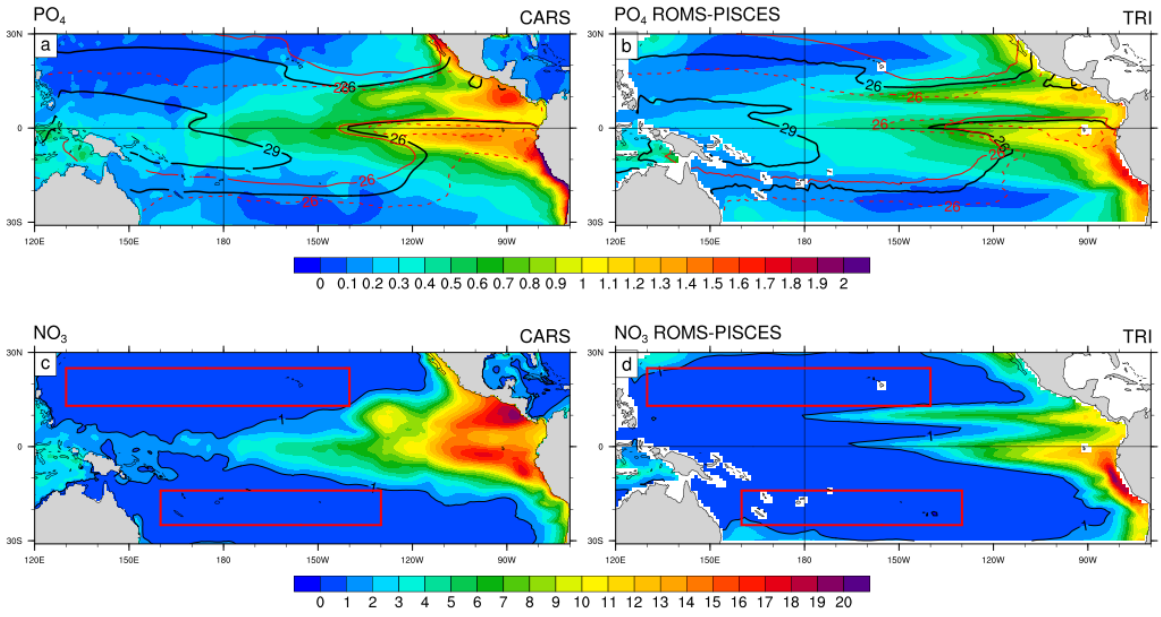
PO4
CARS
a
PO4 ROMS-PISCES
TRI
b
NO3
CARS
c
NO3 ROMS-PISCES
TRI
d
30N
0
30S
120E
150E
180
150W
120W
90W
26
29
0 0.1 0.2 0.3 0.4 0.5 0.6 0.7 0.8 0.9 1 1.1 1.2 1.3 1.4 1.5 1.6 1.7 1.8 1.9 2
0 1 2 3 4 5 6 7 8 9 10 11 12 13 14 15 16 17 18 19 20

Figure 1

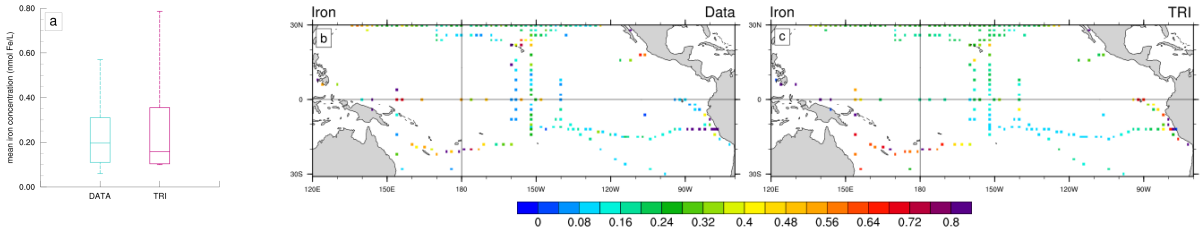
a
mean iron concentration (nmol Fe/L)
0.80
0.60
0.40
0.20
0.00
DATA
TRI
Iron
Data
b
30N
0
30S
120E
150E
180
150W
120W
90W
Iron
TRI
c
0
0.08
0.16
0.24
0.32
0.4
0.48
0.56
0.64
0.72
0.8

Figure 2

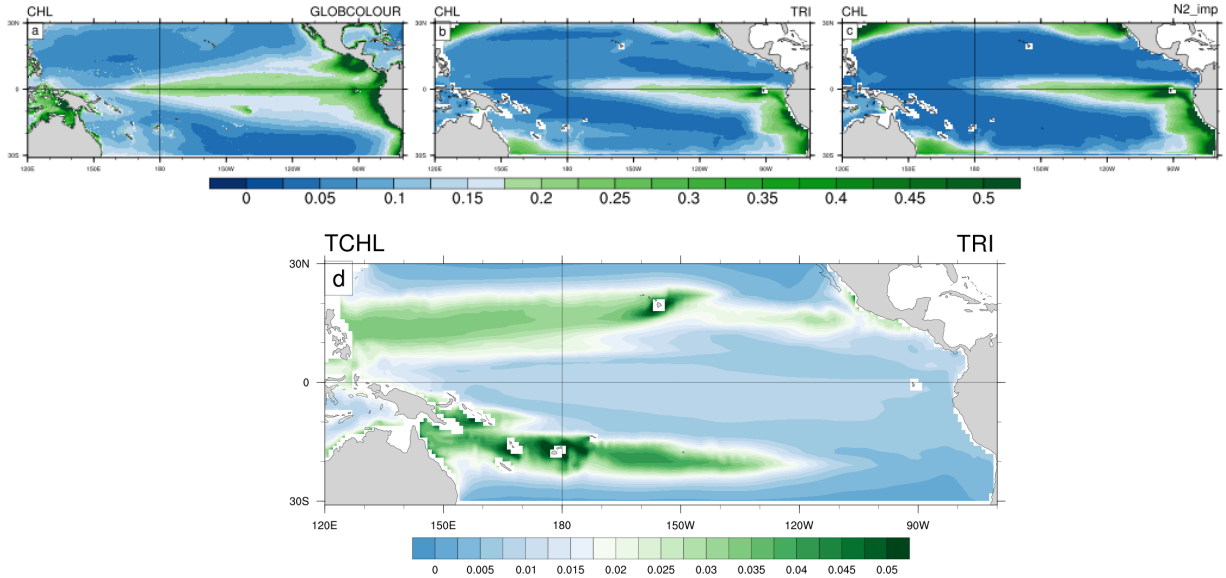
CHL
GLOBCOLOUR
a
CHL
TRI
b
CHL
N2_imp
c
0
0.05
0.1
0.15
0.2
0.25
0.3
0.35
0.4
0.45
0.5
TCHL
TRI
d
30N
0
30S
120E
150E
180
150W
120W
90W
0
0.005
0.01
0.015
0.02
0.025
0.03
0.035
0.04
0.045
0.05

Figure 3

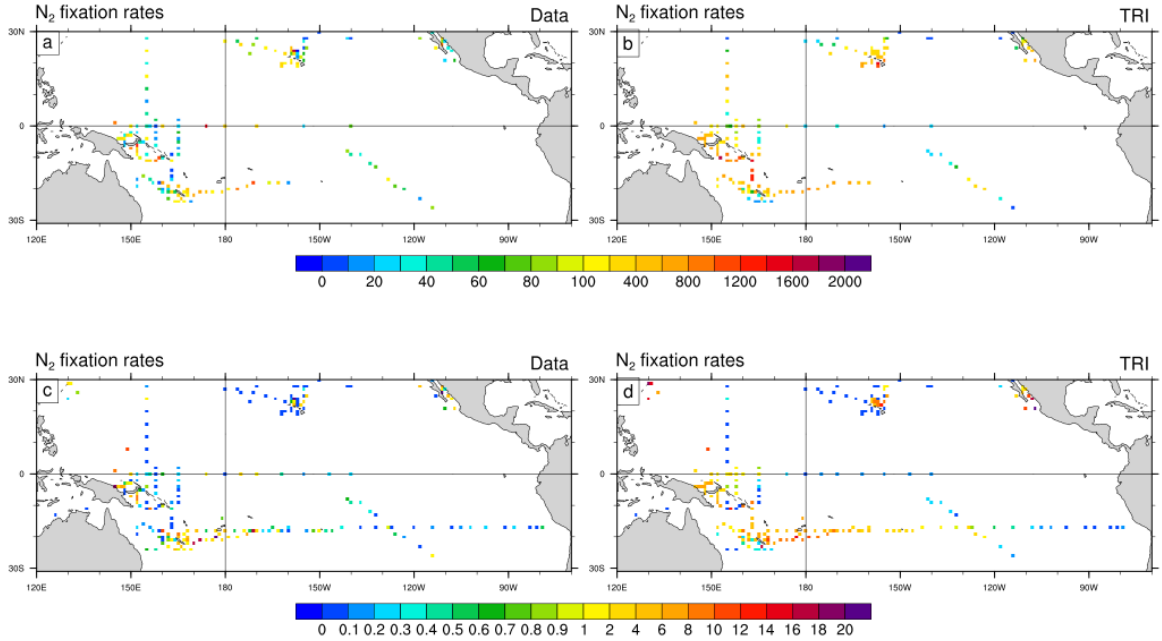
N2 fixation rates
Data
a
N2 fixation rates
TRI
b
30N
0
30S
120E
150E
180
150W
120W
90W
0 20 40 60 80 100 400 800 1200 1600 2000
N2 fixation rates
Data
c
N2 fixation rates
TRI
d
0 0.1 0.2 0.3 0.4 0.5 0.6 0.7 0.8 0.9 1 2 4 6 8 10 12 14 16 18 20

Figure 4

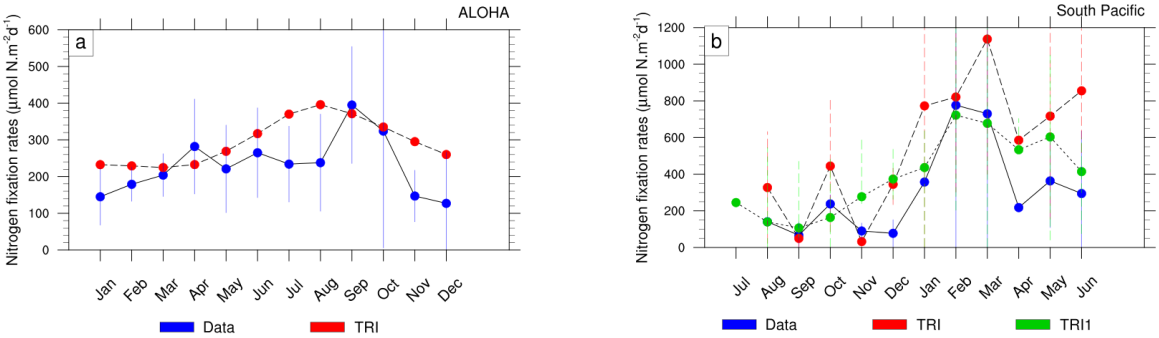
ALOHA
a
Nitrogen fixation rates (µmol N.m-2.d-1)
0
100
200
300
400
500
600
Jan
Feb
Mar
Apr
May
Jun
Jul
Aug
Sep
Oct
Nov
Dec
Data
TRI
South Pacific
b
Nitrogen fixation rates (µmol N.m-2.d-1)
0
200
400
600
800
1000
1200
Jul
Aug
Sep
Oct
Nov
Dec
Jan
Feb
Mar
Apr
May
Jun
Data
TRI
TRI1

Figure 5

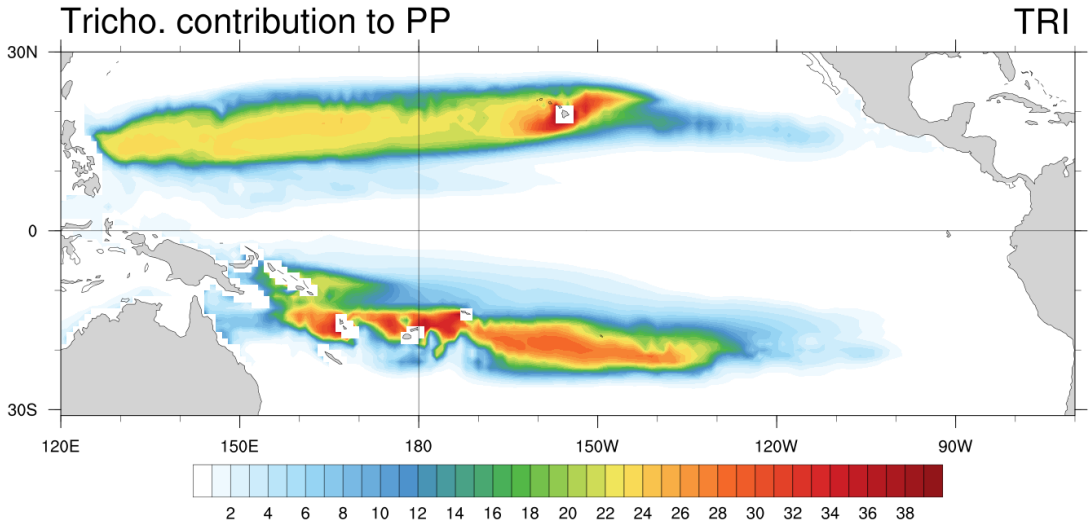
Tricho. contribution to PP
TRI
30N
0
30S
120E
150E
180
150W
120W
90W
2
4
6
8
10
12
14
16
18
20
22
24
26
28
30
32
34
36
38

Figure 6

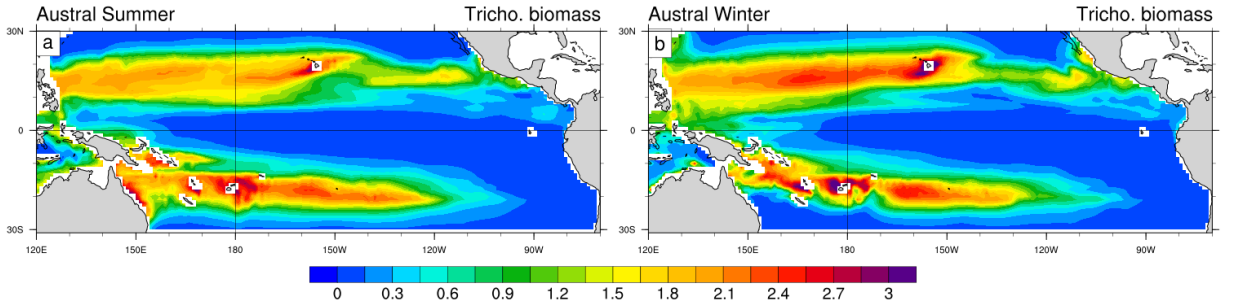
Austral Summer
Tricho. biomass
a
Austral Winter
Tricho. biomass
b
30N
0
30S
120E
150E
180
150W
120W
90W
0
0.3
0.6
0.9
1.2
1.5
1.8
2.1
2.4
2.7
3

Figure 7

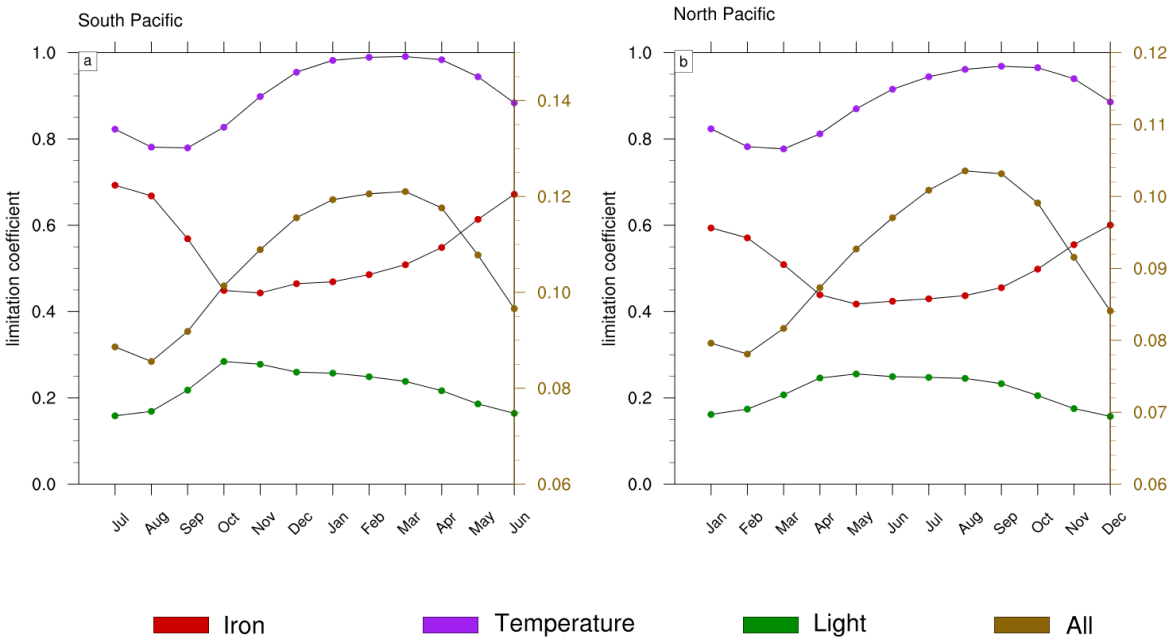
South Pacific
North Pacific
a
b
limitation coefficient
1.0
0.8
0.6
0.4
0.2
0.0
0.14
0.12
0.10
0.08
0.06
0.11
0.09
0.07
Jul
Aug
Sep
Oct
Nov
Dec
Jan
Feb
Mar
Apr
May
Jun
Iron
Temperature
Light
All

Figure 8

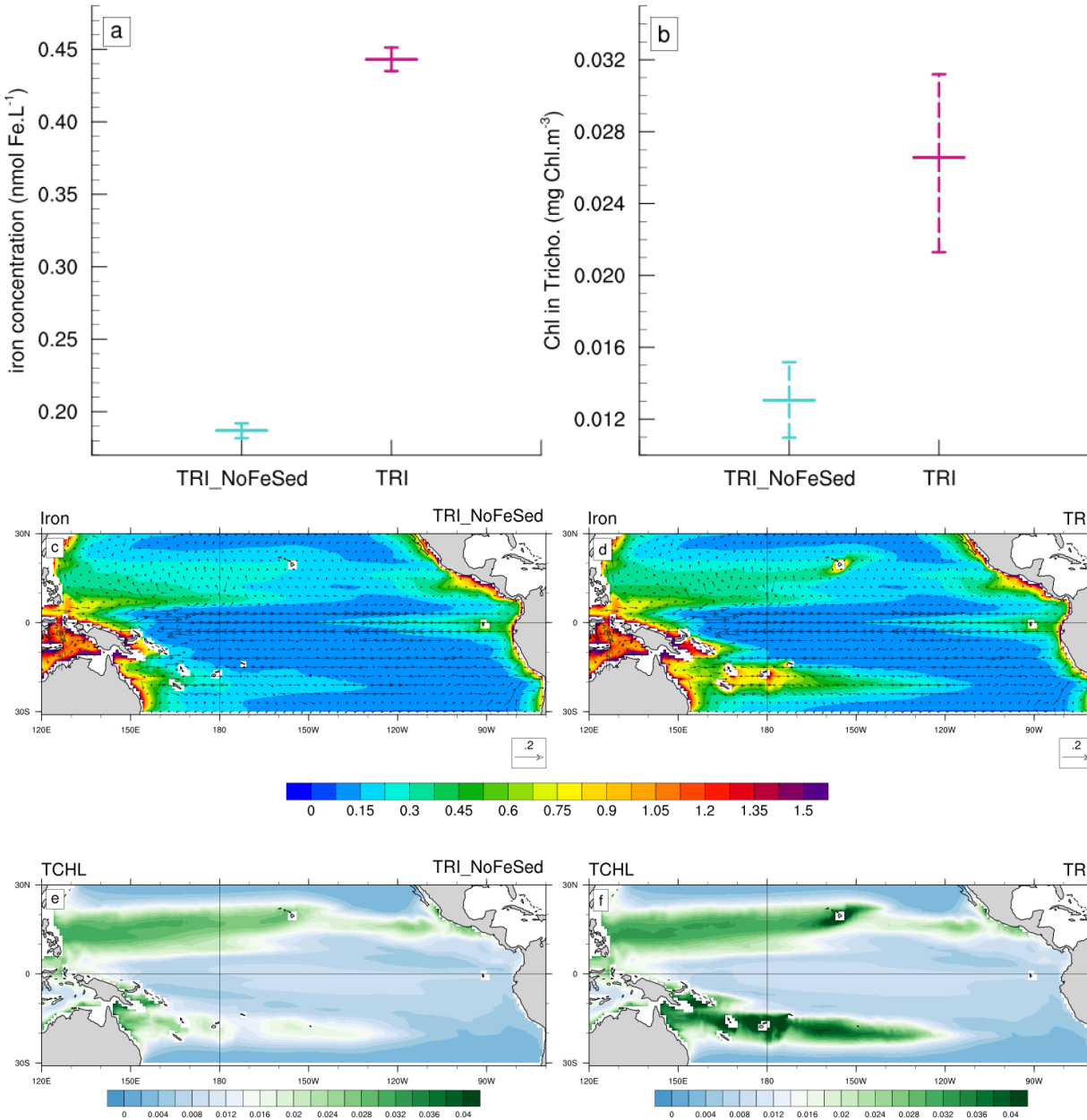
a
iron concentration (nmol Fe.L-1)
0.45
0.40
0.35
0.30
0.25
0.20
TRI_NoFeSed
TRI
b
Chl in Tricho. (mg Chl.m-3)
0.032
0.028
0.024
0.020
0.016
0.012
TRI_NoFeSed
TRI
Iron
TRI_NoFeSed
c
Iron
TRI
d
30N
0
30S
120E
150E
180
150W
120W
90W
.2
0
0.15
0.3
0.45
0.6
0.75
0.9
1.05
1.2
1.35
1.5
TCHL
TRI_NoFeSed
e
TCHL
TRI
f
0
0.004
0.008
0.012
0.016
0.02
0.024
0.028
0.032
0.036
0.04

Figure 9

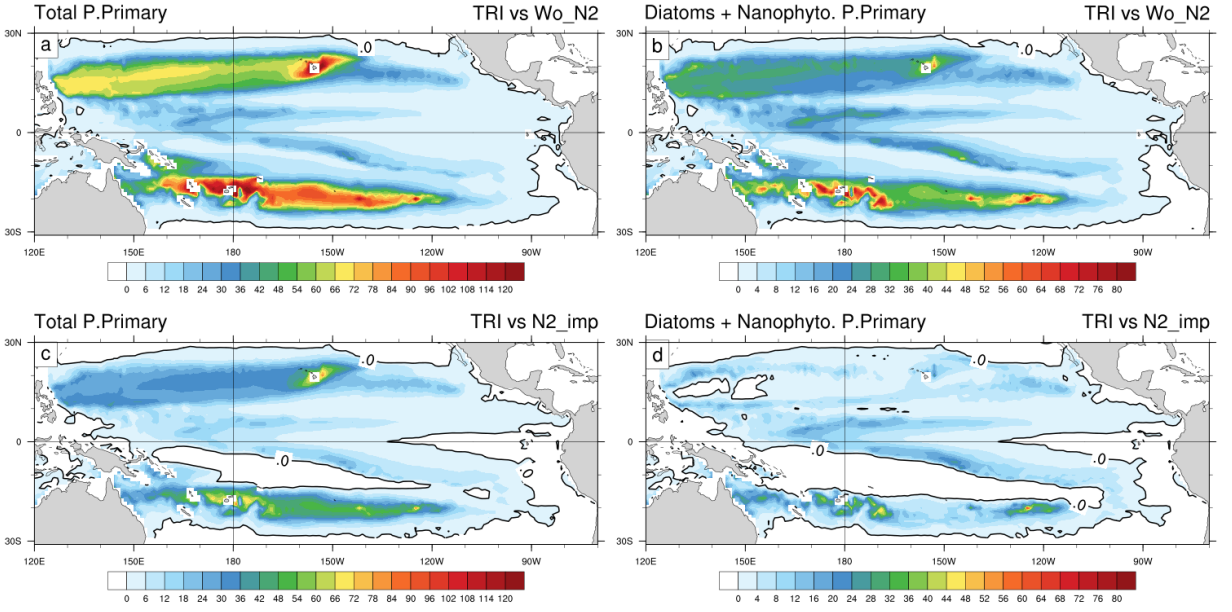
Total P.Primary
TRI vs Wo_N2
a
Diatoms + Nanophyto. P.Primary
TRI vs Wo_N2
b
Total P.Primary
TRI vs N2_imp
c
Diatoms + Nanophyto. P.Primary
TRI vs N2_imp
d
30N
0
30S
120E
150E
180
150W
120W
90W
0 6 12 18 24 30 36 42 48 54 60 66 72 78 84 90 96 102 108 114 120
0 4 8 12 16 20 24 28 32 36 40 44 48 52 56 60 64 68 72 76 80

Figure 10